

# Charge-Separated and Molecular Heterobimetallic Rare Earth–Rare Earth and Alkaline Earth–Rare Earth Aryloxo Complexes Featuring Intramolecular Metal–π-arene Interactions

Glen B. Deacon,\*<sup>[a]</sup> Peter C. Junk,\*<sup>[a]</sup> Graeme J. Moxey,<sup>[a]</sup> Karin Ruhlandt-Senge,\*<sup>[b]</sup> Courtney St. Prix,<sup>[b]</sup> and Maria F. Zuniga<sup>[b]</sup>

**Abstract:** Treatment of a rare earth metal ( $\text{Ln}$ ) and a potential divalent rare earth metal ( $\text{Ln}'$ ) or an alkaline earth metal ( $\text{Ae}$ ) with 2,6-diphenylphenol ( $\text{HOdpp}$ ) at elevated temperatures ( $200\text{--}250^\circ\text{C}$ ) afforded heterobimetallic aryloxo complexes, which were structurally characterised. A charge-separated species  $[(\text{Ln}'/\text{Ae})_2(\text{Odpp})_3][\text{Ln}-(\text{Odpp})_4]$  was obtained for a range of metals, demonstrating the similarities between the chemistry of the divalent rare earth metals and the alkaline earth metals. The  $[(\text{Ln}'/\text{Ae})_2(\text{Odpp})_3]^+$  cation in the heterobimetallic structures is unusual in that it consists solely of bridging aryloxide ligands. A molecular heterobimetallic species  $[\text{AeEu}-(\text{Odpp})_4]$  ( $\text{Ae}=\text{Ca}, \text{Sr}, \text{Ba}$ ) was ob-

tained by treating an alkaline earth metal and Eu metal with  $\text{HOdpp}$  at elevated temperatures. Similarly,  $[\text{BaSr}-(\text{Odpp})_4]$  was prepared by treating Ba metal and Sr metal with  $\text{HOdpp}$ . Treatment of  $[\text{Ba}_2(\text{Odpp})_4]$  with  $[\text{Mg}-(\text{Odpp})_2(\text{thf})_2]$  in toluene afforded  $[\text{Ba}_2(\text{Odpp})_3][\text{Mg}(\text{Odpp})_3(\text{thf})]$ . Analogous solution-based syntheses were not possible for  $[(\text{Ln}'/\text{Ae})_2(\text{Odpp})_3][\text{Ln}-(\text{Odpp})_4]$  complexes, for which the free-metal route was essential. As a result of the absence of additional

**Keywords:** alkaline earth metals • heterobimetallic complexes • O ligands • π interactions • rare earths

donor ligands, the crystal structures of the heterobimetallic complexes feature extensive  $\pi$ -Ph–metal interactions involving the pendant phenyl groups of the Odpp ligands, thus enabling the large electropositive metal atoms to attain coordination saturation. The charge-separated heterobimetallic species were purified by extraction with toluene/thf mixtures at ambient temperature (Ba-containing compounds) or by extraction with toluene under pressure above the boiling point of the solvent (other products). In donor solvents, heterobimetallic complexes other than those containing barium were found to fragment into homometallic species.

## Introduction

Mixed-oxidation-state (II/III) rare earth metal–organic compounds are quite rare, though they continue to increase in number.<sup>[1–11]</sup> Amongst this class,  $[\text{Yb}_2^{\text{II}}(\text{Odpp})_3]^+[\text{Yb}^{\text{III}}(\text{Odpp})_4]^-$  (**1**; Odpp=2,6-diphenylphenolate), which is prepared by direct reaction of Yb metal with the phenol, is unusual because of its charge-separated nature and because the cation contains solely bridging aryloxide ligands.<sup>[11]</sup> This structural feature has otherwise been seen only in the molecular bimetallic complexes  $[\text{LiSn}(\text{Odpp})_3]$ ,<sup>[12]</sup>  $[\text{MGe}-(\text{Odpp})_3]$  ( $\text{M}=\text{Li}\rightarrow\text{Rb}$ )<sup>[13]</sup> and the recently prepared  $[\text{MAe}-(\text{Odpp})_3]$  ( $\text{M}=\text{Na, K, Cs}; \text{Ae}=\text{Ca, Sr, Ba}$ ).<sup>[14,15]</sup> An intriguing possibility is that **1** could be the forerunner of a new class of mixed-oxidation-state heterobimetallic complexes, namely,  $[\text{Ln}'_2^{\text{II}}(\text{Odpp})_3][\text{Ln}^{\text{III}}(\text{Odpp})_4]$  ( $\text{Ln}'=\text{Eu, Sm, Yb}; \text{Ln}=\text{any rare earth element}$ ). Furthermore, from the similar

[a] Prof. Dr. G. B. Deacon, Prof. Dr. P. C. Junk, G. J. Moxey

School of Chemistry  
Monash University  
Clayton, VIC 3800 (Australia)  
Fax: (+61)399054597

E-mail: glen.deacon@sci.monash.edu.au  
peter.junk@sci.monash.edu.au

[b] Prof. Dr. K. Ruhlandt-Senge, Dr. C. St. Prix, Dr. M. F. Zuniga

Department of Chemistry  
1-014 Center for Science and Technology  
Syracuse University  
Syracuse, NY 13244-4100 (USA)  
Fax: (+1)315-443-4070

E-mail: kruhland@syr.edu

 Supporting information for this article is available on the WWW under <http://dx.doi.org/10.1002/chem.200900229>.

ity of the  $\text{Ca}^{2+}/\text{Yb}^{2+}$  and  $\text{Sr}^{2+}/\text{Eu}^{2+}$  ionic radii,<sup>[16]</sup> the mixed oxidation class might be extended to  $[\text{Ae}_2(\text{Odpp})_3][\text{Ln}(\text{Odpp})_4]$  ( $\text{Ae}=\text{Ca}, \text{Sr}, \text{Ba}$ ) complexes. Moreover, the similarities between the structures of  $[\text{Yb}_2(\text{Odpp})_4]^{[11]}$  and  $[\text{Ca}_2(\text{Odpp})_4]^{[17]}$  and between the structures of  $[\text{Eu}_2(\text{Odpp})_4]^{[11]}$  and  $[\text{Ae}_2(\text{Odpp})_4]$  ( $\text{Ae}=\text{Sr}, \text{Ba}$ )<sup>[17]</sup> suggest that a new class of neutral divalent heterobimetallic species  $[\text{AeLn}(\text{Odpp})_4]$  might also be accessible. We now report the preparation and structural characterisation of a new class of mixed-oxidation-state heterobimetallic compounds  $[(\text{Ln}'/\text{Ae})_2(\text{Odpp})_3][\text{Ln}(\text{Odpp})_4]$ , and the molecular heterobimetallic species  $[\text{AeEu}(\text{Odpp})_4]$  ( $\text{Ae}=\text{Ca}, \text{Sr}, \text{Ba}$ ) by the simple reaction of an appropriate mixture of metallic elements with 2,6-diphenylphenol (HODpp) at elevated temperatures. The wide range of products obtained establishes the general significance and value of the synthetic method, which is potentially applicable to further combinations of Ln and Ae elements with the present ligand, to analogous bimetallics with other phenolate and plausibly organoamide ligands, and indeed to different combinations of elements, such as Ae/Ae', as shown by the preparation of  $[\text{BaSr}(\text{Odpp})_4]$ .

A major problem posed by **1** that is also applicable to many of the present charge-separated complexes is insolubility in non-polar solvents and dissociation into homometallic species in polar solvents, evidently requiring hand-picking to separate the target bimetallics from residual metal. However, a major advance has been the purification of representative compounds by crystallisation from toluene under pressure well above the boiling point of the solvent to avoid fragmentation by polar solvents. In addition,  $[\text{Ba}_2(\text{Odpp})_3]^{+}$ -containing complexes can uniquely be crystallised from toluene/thf without decomposition into the homometallic species.

Rare earth and heavier alkaline earth aryloxides and alkoxides are of considerable contemporary interest and have led to a number of reviews and perspective articles,<sup>[18,19]</sup> with particular interest in their structural chemistry<sup>[19]</sup> and uses in metal–organic chemical vapour deposition, atomic layer deposition and sol-gel applications,<sup>[20]</sup> and they make a significant contribution to a key monograph.<sup>[21]</sup> The present complexes add two new exciting structural classes that can be potentially generalised to other aryloxide and organoamide systems. A feature of the structures of the present complexes is extensive intramolecular  $\pi$ -Ph–Ln'/Ae bonding. The  $\pi$  bonding of neutral ligands to lanthanoids is well known in zero-, di- and trivalent arene–lanthanoid complexes<sup>[22a,b]</sup> and inter- and intramolecular  $\pi$  bonding of aryl groups to Ln (and Ae) elements is an increasing phenomenon.<sup>[22a,c,d]</sup>

## Results and Discussion

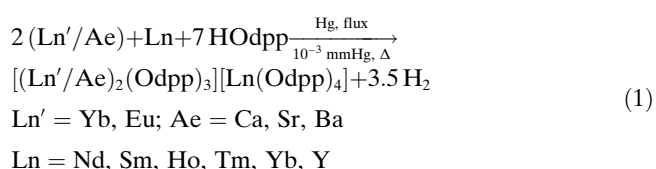
**Syntheses:** Treatment of two rare earth metals, of which one is Yb or Eu, or a combination of a rare earth metal and a heavy alkaline earth metal (Ca, Sr, Ba) with HODpp at 200–250°C in an evacuated and sealed Carius tube afforded

charge-separated heterobimetallic 2,6-diphenylphenolate complexes  $[(\text{Ln}'/\text{Ae})_2(\text{Odpp})_3][\text{Ln}(\text{Odpp})_4]$  (Equation (1); Table 1).

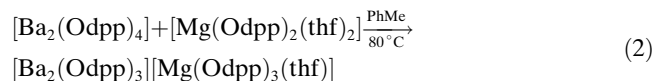
Table 1. List of heterobimetallic compounds and reaction/work-up conditions employed.

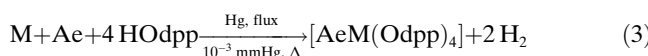
Compound	Number	Conditions <sup>[a]</sup>	Flux <sup>[b]</sup>
$[\text{Yb}_2(\text{Odpp})_3][\text{Yb}(\text{Odpp})_4]$	<b>1a, 1b</b>	A	E
$[\text{Yb}_2(\text{Odpp})_3][\text{Y}(\text{Odpp})_4]\cdot 2\text{PhMe}$	<b>2</b> ·2 PhMe	C	E
$[\text{Yb}_2(\text{Odpp})_3][\text{Y}(\text{Odpp})_4]\cdot 0.5\text{PhMe}$	<b>2</b> ·0.5 PhMe	B	E
$[\text{Yb}_2(\text{Odpp})_3][\text{Y}(\text{Odpp})_4]\cdot 1.5\text{PhMe}$	<b>2</b> ·1.5 PhMe	B	E
$[\text{Eu}_2(\text{Odpp})_3][\text{Y}(\text{Odpp})_4]$	<b>3</b>	A	F
$[\text{Eu}_2(\text{Odpp})_3][\text{Y}(\text{Odpp})_4]\cdot 0.5\text{PhMe}$	<b>3</b> ·0.5 PhMe	B	F
$[\text{Eu}_2(\text{Odpp})_3][\text{Nd}(\text{Odpp})_4]$	<b>4</b>	A	F
$[\text{Eu}_2(\text{Odpp})_3][\text{Ho}(\text{Odpp})_4]$	<b>5</b>	A	F
$[\text{Ca}_2(\text{Odpp})_3][\text{Nd}(\text{Odpp})_4]\cdot \text{PhMe}$	<b>6</b> ·PhMe	C, B	E, F <sup>[c]</sup>
$[\text{Ca}_2(\text{Odpp})_3][\text{Ho}(\text{Odpp})_4]$	<b>7</b>	A, B	E, F <sup>[d]</sup>
$[\text{Ca}_2(\text{Odpp})_3][\text{Tm}(\text{Odpp})_4]$	<b>8</b>	A	E
$[\text{Ca}_2(\text{Odpp})_3][\text{Yb}(\text{Odpp})_4]$	<b>9</b>	A	G
$[\text{Sr}_2(\text{Odpp})_3][\text{Nd}(\text{Odpp})_4]\cdot 0.5\text{PhMe}$	<b>10</b> ·0.5 PhMe	B	F
$[\text{Sr}_2(\text{Odpp})_3][\text{Ho}(\text{Odpp})_4]\cdot 0.5\text{PhMe}$	<b>11</b> ·0.5 PhMe	B	F
$[\text{Ba}_2(\text{Odpp})_3][\text{Sm}(\text{Odpp})_4]$	<b>12</b>	B	F
$[\text{Ba}_2(\text{Odpp})_3][\text{Sm}(\text{Odpp})_4]\cdot \text{PhMe}$	<b>12</b> ·PhMe	D	F
$[\text{Ba}_2(\text{Odpp})_3][\text{Sm}(\text{Odpp})_4]\cdot 4\text{PhMe}$	<b>12</b> ·4 PhMe	D	F
$[\text{Ba}_2(\text{Odpp})_3][\text{Yb}(\text{Odpp})_4]$	<b>13</b>	A, D	F
$[\text{Ba}_2(\text{Odpp})_3][\text{Mg}(\text{Odpp})_3(\text{thf})]$	<b>14</b>	C	E
$[\text{CaEu}(\text{Odpp})_4]\cdot \text{PhMe}$	<b>15</b> ·PhMe	C	F
$[\text{SrEu}(\text{Odpp})_4]$	<b>16</b>	A	F
$[\text{SrEu}(\text{Odpp})_4]\cdot \text{PhMe}$	<b>16</b> ·PhMe	C	F
$[\text{BaSr}(\text{Odpp})_4]$	<b>17</b>	A, D	F
$[\text{BaEu}(\text{Odpp})_4]$	<b>18</b>	D	F
$[\text{BaEu}(\text{Odpp})_4]\cdot \text{PhMe}$	<b>18</b> ·PhMe	D	F

[a] A = crystals obtained directly from tube; B = crystals obtained by high-pressure toluene recrystallisation; C = crystals obtained from toluene at ambient temperature or at –20°C after prolonged storage; D = crystals obtained from toluene/thf. [b] E = no flux; F = 1,3,5-tri-*tert*-butylbenzene; G = 1,2,4,5-tetramethylbenzene. [c] Fluxes E and F were used with conditions C and B, respectively. [d] Fluxes E and F were used with conditions A and B, respectively.



Contrastingly, heterobimetallic alkaline earth complex  $[\text{Ba}_2(\text{Odpp})_3][\text{Mg}(\text{Odpp})_3(\text{thf})]$  **14** was prepared by treating  $[\text{Ba}_2(\text{Odpp})_4]$  with  $[\text{Mg}(\text{Odpp})_2(\text{thf})_2]$  in toluene [Eq. (2)], a synthesis that did not succeed for  $[(\text{Ln}'/\text{Ae})_2(\text{Odpp})_3][\text{Ln}(\text{Odpp})_4]$  complexes. Treatment of Eu metal and an alkaline earth metal with HODpp afforded a dinuclear molecular heterobimetallic species  $[\text{AeEu}(\text{Odpp})_4]$  [Eq. (3)] ( $\text{Ae}=\text{Ca}$  **15**;  $\text{Sr}$  **16**;  $\text{Ba}$  **18**). Similarly, treatment of Sr metal and Ba metal with HODpp afforded  $[\text{BaSr}(\text{Odpp})_4]$  **17** [Eq. (3)]. Table 1 contains a summary of the complexes synthesised and the reaction conditions and work-up methods employed.





M = Eu, Ae = Ca/Sr/Ba; M = Sr, Ae = Ba.

Direct metalation is a conceptually simple synthetic route to homoleptic heterobimetallic species. An added benefit is that no air-sensitive reagents need to be prepared. The simple structural frameworks and homoleptic nature of heterobimetallic complexes **1–18** contrast with previously reported solvated aryloxo rare earth–alkaline earth heterobimetallic complexes, such as  $[\text{H}_2\text{Ba}_2\text{Sr}_6(\text{hmpa})_6(\mu_5\text{-O}_2)(\text{OPh})_{14}]$  ( $\text{hmpa} = \text{hexamethylphosphoramide}$ ),<sup>[23a]</sup>  $[\text{H}_2\text{Eu}_2\text{Ba}_6(\mu_5\text{-O}_2)(\text{O}i\text{Pr})_{16}(\text{thf})_4]$ <sup>[23b]</sup> and  $[\text{EuBa}_2\text{Sr}_6(\text{dig})_2(\text{dme})(\text{OAr}')_7]$  ( $\text{OAr}' = 4\text{-methylphenolate}$ , dig = diglyme, dme = 1,2-dimethoxyethane,<sup>[23b]</sup> and the solvated alkali metal–alkaline earth and alkali metal–rare earth mixed metal cages  $[\text{MM}'(\text{OPh})_8(\text{thf})_6]$  (M = Ca, Sr, Ba, Sm, Eu; M' = Li, Na).<sup>[24]</sup>

Although molten HOdpp (m.p. 101–103 °C) may act as a solvent during the initial sequence of the metal-based reactions for the syntheses of **1–13** and **15–18**, fluxes (1,2,4,5-tetramethylbenzene or 1,3,5-tri-*tert*-butylbenzene) were added to most reaction mixtures to promote metal–phenol contact and crystallisation of the products (see below). Mercury was added to the reaction mixtures to assist the reaction by cleaning the metal surface and to activate the metals by forming an amalgam. Mercury was previously employed in the synthesis of  $[\text{M}_2(\text{Odpp})_4]$  (M = Ca, Sr, Ba, Eu, Yb) and the synthesis of **1**, and the reaction with Yb metal was incomplete without mercury even at higher temperatures.<sup>[11]</sup> The preparation of charge-separated complexes **12** and **13** without mercury was attempted, but only the homometallic species  $[\text{Ba}_2(\text{Odpp})_4]$  was isolated along with a large amount of unreacted (presumably rare earth) metal, even after prolonged reaction times. This is not surprising given that Ba metal is more electropositive than Sm and Yb. However, the preparation of molecular bimetallics **17** and **18** proceeded smoothly without mercury. Possibly, these soluble species are more readily formed than the ionic complexes, and/or the reactivities of the pairs of metals (Ba/Sr and Ba/Eu) are better matched. In a similar vein, mercury activation was not required in the synthesis of heterobimetallic alkali metal–alkaline earth metal Odpp complexes, though these syntheses generally did not involve two free metals.<sup>[14,15]</sup>

Differential reactivity of the two metals, either intrinsic or arising from the nature of the metal filings, created problems generally and not just in reactions without mercury. Initial attempts to prepare  $[\text{Yb}_2(\text{Odpp})_3][\text{Y}(\text{Odpp})_4]$  **2** gave crystals of homometallic **1**, even when using a considerable excess of Y metal, as did an attempt to produce a Yb/Eu bimetallic complex. Repeating the Yb/Y synthesis by using similar conditions, but with some variations in the work-up, gave the bimetallic as various toluene solvates, **2·2PhMe**, **2·0·5PhMe** (with 25:75 Yb/Y disorder in the anion) and **2·1·5PhMe** from two preparations. Greater consistency was achieved in the other syntheses, which were generally carried out in the presence of 1,3,5-tri-*tert*-butylbenzene as a flux. Because of the difficulties encountered in the synthesis

of **2**, most syntheses of  $[(\text{Ln}'/\text{Ae})_2(\text{Odpp})_3][\text{Ln}(\text{Odpp})_4]$  complexes utilised a considerable excess of Ln. A smaller excess was employed in reactions involving Ba, which were also carried out under somewhat more aggressive conditions (temperature/time). Nevertheless, Ca/Nd and Ca/Ho complexes **6** and **7**, having initially been prepared with Ca/Ln ratios of 1:4 and no flux, were subsequently prepared from near stoichiometric amounts of the two metals in a 1,3,5-tri-*tert*-butylbenzene flux. Although  $[\text{Ca}_2(\text{Odpp})_3][\text{Tm}(\text{Odpp})_4]$  **8** was characterised as a hand-picked single crystal, the synthesis could not be repeated. Use of a large excess of Ln led in some cases to formation of  $[\text{Ln}(\text{Odpp})_3]$  (e.g., Ln = Nd, Sm **21**; Ho, Tm **20**) accompanying the  $[(\text{Ln}'/\text{Ae})_2(\text{Odpp})_3][\text{Ln}(\text{Odpp})_4]$  bimetallic complex, but was easily removed owing to its high solubility in cold toluene. By contrast, the molecular bimetallics  $[\text{AeEu}(\text{Odpp})_4]$  (Ae = Ca, Sr, Ba) and  $[\text{BaSr}(\text{Odpp})_4]$  **15–18** were prepared with stoichiometric amounts of the two metals, but  $[\text{AeEu}(\text{Odpp})_4]$  (Ae = Ca, Sr) showed a degree of metal-atom disorder in the structures with an overall excess of Ae in the single crystals examined. An attempt to prepare the neutral bimetallic  $[\text{CaYb}(\text{Odpp})_4]$  gave single crystals of the charge-separated  $[\text{Ca}_2(\text{Odpp})_3][\text{Yb}(\text{Odpp})_4]$  **9**, but with Ca/Yb 75:25 disorder in the cation positions that indicated a Yb-rich product, whereas an attempt to prepare  $[\text{CaSr}(\text{Odpp})_4]$  failed with only a homometallic complex isolated. It is also interesting that a 1:1 ratio of Ba metal and a rare earth metal (Ln = Sm, Eu, Yb) to four equivalents of HOdpp consistently afforded the heterobimetallic molecular species  $[\text{BaEu}(\text{Odpp})_4]$  **18** for Ln = Eu, but for Sm and Yb the charge-separated heterobimetallic species  $[\text{Ba}_2(\text{Odpp})_3][\text{Ln}(\text{Odpp})_4]$  (Ln = Sm (**12**), Yb (**13**)) was formed, commensurate with the decreased stability of the divalent oxidation state for Sm and Yb compared with Eu.

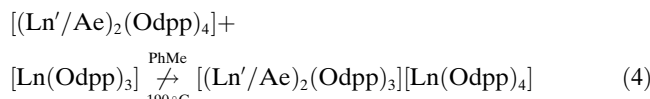
After direct reaction of the metals with HOdpp, X-ray quality crystals of the target complexes could often be hand-picked directly from the Carius tube (Table 1). However, unreacted metal and small amounts of homometallic co-products were present in reaction mixtures, necessitating solvent extraction to obtain pure bulk samples of the target complexes. The charge-separated heterobimetallic complexes have an extremely low solubility in non-coordinating solvents, even hot toluene, precluding their use as an extractant for these complexes. They are also extremely insoluble in diethyl ether. Except in the case of  $[\text{Ba}_2(\text{Odpp})_3][\text{Ln}(\text{Odpp})_4]$  complexes (see below), use of thf as an extractant led to dissociation of  $[(\text{Ln}'/\text{Ae})_2(\text{Odpp})_3][\text{Ln}(\text{Odpp})_4]$  into homometallic complexes, as exemplified by **1** and **6** (see below). Accordingly, to obtain pure bulk samples of the heterobimetallic charge-separated complexes, two work-up procedures were employed:

- Following extraction of the homometallic species from the reaction product with toluene, the representative charge-separated complexes **2**, **3**, **6**, **7**, **10–12** were extracted from the metal-containing residue by toluene under pressure at 190 °C, well above the boiling point of

this solvent (see the Experimental Section for details). Very slow cooling gave crystalline material, often with single crystals of toluene solvates. The method takes advantage of the high thermal stability of these compounds (*m.p.* > 250 °C) and enabled the yields of the compounds to be determined.

- 2) The  $[\text{Ba}_2(\text{Odpp})_3][\text{Ln}(\text{Odpp})_4]$  complexes could be successfully extracted by and crystallised from toluene/thf (see the Experimental Section) without irreversible dissociation into homometallic species. On the other hand, the more soluble *neutral* heterobimetallic species  $[\text{AeEu}(\text{Odpp})_4]$  ( $\text{Ae} = \text{Ca}$  **15**;  $\text{Sr}$  **16**) were extracted with warm toluene, but  $[\text{BaEu}(\text{Odpp})_4]$  **18** and  $[\text{BaSr}(\text{Odpp})_4]$  **17** were much less soluble in toluene and were extracted with a toluene/thf mixture. However, use of this solvent mixture after an attempted preparation of  $[\text{CaSr}(\text{Odpp})_4]$  led to isolation of  $[\text{Sr}(\text{Odpp})_2(\text{thf})_3]$  **22**. Thus, amongst the present complexes, most barium-containing bimetallic complexes are uniquely stable to toluene/thf with the exception of  $[\text{Ba}_2(\text{Odpp})_3][\text{Mg}(\text{Odpp})_3(\text{thf})]$  **14** (see below).

Despite the insolubility of *isolated*  $[(\text{Ln}'/\text{Ae})_2(\text{Odpp})_3][\text{Ln}(\text{Odpp})_4]$  complexes in toluene at room temperature, small amounts of single crystals of **2·2PhMe** and **6·PhMe** were deposited on prolonged standing from toluene that had been used to extract homometallic species from the bulk charge-separated products. Thus, the blue washings from a synthesis of **6** initially deposited crystals of  $[\text{Nd}(\text{Odpp})_3]$ , and on further standing at -20 °C the solution turned green and a few crystals of **6·PhMe** were also obtained. Previously, bulk **1** has been shown to give single crystals of **1·PhMe** under toluene for several weeks. Possibly the  $[(\text{Ln}'/\text{Ae})_2(\text{Odpp})_3][\text{Ln}(\text{Odpp})_4]$  complexes have very slight solubility in toluene, or they can equilibrate with the corresponding homometallic derivatives. However, attempts to prepare **2** and **6** by heating the homometallic counterparts in toluene have failed so far, even at 190 °C followed by slow cooling and prolonged standing [Eq. (4)]. Earlier, an attempt to prepare **1·PhMe** from  $[\text{Yb}_2(\text{Odpp})_4]$  and  $[\text{Yb}(\text{Odpp})_3]$  in boiling toluene was unsuccessful.<sup>[11]</sup> In contrast, the Ae'/Ae complex  $[\text{Ba}_2(\text{Odpp})_3][\text{Mg}(\text{Odpp})_3(\text{thf})]$  was obtained by treatment of  $[\text{Ba}_2(\text{Odpp})_4]$  with  $[\text{Mg}(\text{Odpp})_2(\text{thf})_2]$  in toluene [Eq. (2)], but the synthesis failed in toluene/thf 1:1. This is the sole system with an anion of a divalent metal.



Ae = Ca; Ln' = Yb; Ln = Nd, Y

**Characterisation:** Whilst X-ray crystallography provided the primary characterisation, especially in the case of hand-picked single crystals, the two extraction methods (above) provided bulk samples of the charge-separated complexes for yield determination, infrared spectroscopy and micro-

analyses and/or metal analysis in representative cases. Satisfactory elemental analyses were generally obtained both for these compounds and for the soluble uncharged bimetals, occasionally corresponding to loss of toluene of solvation. In the case of **2·0·5PhMe**, in which Yb/Y disorder was observed in the  $[\text{Y}(\text{Odpp})_4]^-$  anions of the single crystals, the analytical data on the bulk sample were closer to the values calculated for the undisordered composition. For complexes **15** and **16**, in which single crystals were Ca- or Sr-rich owing to Ae/Eu disorder, analyses of the bulk product were closer to an undisordered composition for **15** but provided no clear distinction for **16**. All infrared spectra showed the features expected for the Odpp ligand and the absence of a  $\nu(\text{OH})$  absorption was indicative of deprotonation of the phenol. The spectra of the charge-separated species were similar but minor differences at  $\tilde{\nu} = 1600\text{--}1500\text{ cm}^{-1}$  ( $\nu(\text{CC})$ ) may reflect differences in  $\pi\text{-Ph-Ln'/Ae}$  coordination (below).

Meaningful  $^1\text{H}$  NMR spectra were precluded by insolubility in non-polar solvents and dissociation into homometallic species in polar solvents. Thus, the  $^1\text{H}$  NMR spectrum of **6·PhMe** (washed with toluene to remove any homometallic impurities) in  $[\text{D}_8]\text{thf}$  was a composite of those of  $[\text{Ca}_2(\text{Odpp})_4]\text{PhMe}$  and  $[\text{Nd}(\text{Odpp})_3]$  (1:1) in the same medium, but confirmed the composition of the heterobimetallic complex. On a preparative scale, extraction into thf and crystallisation of **6·PhMe** gave the known  $[\text{Nd}(\text{Odpp})_3(\text{thf})_2]\text{-2thf}$  and also colourless crystals that were unsuitable for X-ray studies but likely to be  $[\text{Ca}(\text{Odpp})_2(\text{thf})_3]$ . Extraction of **6·PhMe** with toluene/thf 6:1 gave crystals of  $[\text{Ca}_2(\text{Odpp})_4(\text{thf})_2]$  **19**. This ready break-up of the charge-separated species in polar media was also exemplified by the quantitative recovery of  $[\text{Mg}(\text{Odpp})_2(\text{thf})_2]$  from an attempted synthesis of **14** in toluene/thf 1:1 and isolation of  $[\text{Sr}(\text{Odpp})_2(\text{thf})_3]$  **22** from toluene/thf following an attempted synthesis of  $[\text{CaSr}(\text{Odpp})_4]$ . Similarly, past attempts to prepare Li/Mg/Odpp bimetals in thf or diethyl ether resulted in precipitation of  $[\text{Mg}(\text{Odpp})_2(\text{solvent})_2]$ , whereas heterobimetallic species could be prepared in toluene.<sup>[25]</sup> Furthermore, treatment of  $[\text{CsCa}(\text{Odpp})_3]$  with toluene/thf 1:1 gave  $[\text{Cs}(\text{Odpp})]_n$ <sup>[15]</sup> and similar treatment of **1** gave  $[\text{Yb}_2(\text{Odpp})_4]$  and  $[\text{Yb}(\text{Odpp})_3]$ .<sup>[11]</sup>

Two unexpected colour variations were observed in the products. For example,  $[\text{Ba}_2(\text{Odpp})_3][\text{Sm}(\text{Odpp})]$  **12** hand-picked from the reaction mixture was colourless, but solvates **12·PhMe** and **12·4PhMe** were dark green. Likewise, single crystals of **6·PhMe** deposited from toluene over a prolonged period were dark green, but the bulk microcrystalline compound was the expected blue.

**X-ray crystallography studies:** Crystalline samples of heterobimetallic compounds **1–18**, often as toluene solvates, of suitable quality for X-ray structure determination were either obtained directly from the Carius tube or were grown from toluene (mainly after dissolution at 190 °C) or toluene/thf mixtures (see Table 1 and the Experimental Section). Crystalline samples of homometallic compounds **19–22** were either obtained directly from the Carius tube or grown from

toluene/thf mixtures (see above). Table S1 in the Supporting Information contains a summary of relevant data collection and refinement parameters for all compounds fully characterised by X-ray crystallography. The crystal data of **1a**, **1b**, **2**·0.5PhMe, **2**·1.5PhMe and **8** were not of sufficient quality to discuss bond lengths, but the connectivity of the molecules and identity of the metal atoms was unequivocally determined. Their unit cell data are included with their preparations in the Supporting Information. Complex **11**·0.5PhMe (unit cell data with the synthesis) was found to be isomorphous with **10**·0.5PhMe, so a data collection was not undertaken. The solid-state structures of the heterobimetallic compounds can be classified into two structural types: 1) a charge-separated species containing a  $[(\text{Ln}'/\text{Ae})(\text{Odpp})_3]^+$  cation and either a  $[\text{Ln}(\text{Odpp})_4]^-$  (**1**–**13**) or  $[\text{Mg}(\text{Odpp})_3(\text{thf})]^-$  anion (**14**) or 2) a neutral dinuclear species  $[\text{AeEu}(\text{Odpp})_4]$  **15**, **16**, **18** and  $[\text{BaSr}(\text{Odpp})_4]$  **17**. Selected metal–oxygen bond lengths for all heterobimetallic compounds are listed in Tables 2 and 3. Bond angles are given in Tables S2 and S3 in the Supporting Information. Because the  $[(\text{Ln}'/\text{Ae})_2(\text{Odpp})_3]^+$  cations of **1**–**14** have solely bridging aryloxide ligands, the potentially naked faces of the large metal ions are shrouded by pendant phenyl groups locked in place by  $\pi$ -Ph–Ln'/Ae interactions. Likewise, the low (3,4) coordinate metals in  $[\text{AeEu}(\text{Odpp})_4]$  and  $[\text{BaSr}(\text{Odpp})_4]$  complexes have similar interactions. Details of the  $\pi$ -Ph–Ln'/Ae interactions are given in Tables 4 and 5. In choosing upper limits for significant Ln/Ae···C interactions, we have used Ln/Ae···C bond lengths in dinuclear  $[\text{Ln}(\text{OAr}^2)_2\{\mu-(\text{O}: \eta^6-$

Table 3. Selected bond lengths [Å] in neutral heterobimetallic compounds.

	<b>15</b> ·PhMe	<b>16</b>	<b>16</b> ·PhMe	<b>17</b>	<b>18</b>	<b>18</b> ·PhMe
	M' = Eu	M' = Eu	M' = Eu, M = Sr	M' = Sr	M' = Eu	M' = Eu
	M = Ca	M = Sr	M = Sr	M = Ba	M = Ba	M = Ba
M'1–O1	2.303(3)					
M'1–O2	2.491(3)	2.420(8)	2.417(1)	2.391(4)	2.468(2)	2.393(1)
M'1–O3	2.368(3)	2.417(7)	2.432(2)	2.497(4)	2.384(2)	2.425(2)
M'1–O4		2.444(9)	2.449(2)	2.505(4)	2.488(2)	2.478(2)
M1–O1		2.313(8)	2.36(1)	2.459(4)	2.480(2)	2.495(2)
M1–O2	2.28(1)	2.404(7)	2.43(1)	2.917(4)	2.778(2)	2.931(2)
M1–O3	2.30(1)	2.622(8)	2.50(1)	2.552(4)	2.940(2)	2.623(2)
M1–O4	2.118(9)	2.514(8)	2.50(1)	2.762(4)	2.562(2)	2.840(2)
M'1…M1	3.795(2)	3.586(2)	3.531(2)	3.8075(7)	3.8116(5)	3.8206(5)

$\text{Ar}^2)-\text{OAr}^2]\}_2$  ( $\text{OAr}^2 = 2,6\text{-di-isopropylphenolate}$ ),<sup>[30a,b]</sup> dinuclear  $[\text{Ln}(\text{NHAr}^2)_2\{\mu-(\text{N}: \eta^6-\text{Ar}^2)-\text{NHAr}^2\}]_2$  ( $\text{Ar}^2 = 2,6\text{-di-isopropylphenyl}$ )<sup>[22d]</sup> and polynuclear  $[\text{Ae}(t\text{Bu}_2\text{pz})_2]_n$  ( $\text{Ae} = \text{Ca}$ ,  $n = 3$ ;  $\text{Ae} = \text{Sr}$ ,  $n = 4$ ;  $\text{Ae} = \text{Ba}$ ,  $n = 6$ ;  $t\text{Bu}_2\text{pz} = 3,5\text{-di-tert-butylpyrazolate}$ ) complexes,<sup>[30c]</sup> in which intermolecular  $\pi$ -Ph–Ln/Ae interactions give rise to the dimeric/oligomeric complexes. In addition, there are a number of  $[\text{Ln}/\text{Ae}(\text{Odpp})]$  complexes for which  $\pi$ -Ph–Ln/Ae interactions have been reported,<sup>[11,17,29,35–37]</sup> as well as a limited number of  $[\text{Ln}^{\text{II/III}}\text{(arene)}]^n+$  ( $n = 2,3$ ) complexes<sup>[22]</sup> to assist in deciding bonding limits. Conservative upper limits for Ln/Ae···C bonding have been consistently chosen. A representative detailed justification of limits is given for  $[\text{Yb}_2(\text{Odpp})_3]^+$  below.

Table 2. Selected bond lengths [Å] in charge-separated heterobimetallic compounds.

<b>2</b> ·2PhMe	<b>3</b>	<b>3</b> ·0.5PhMe	<b>4</b>	<b>5</b>	<b>6</b> ·PhMe	<b>7</b>
Ae = Yb Ln = Y	Ae = Eu Ln = Y	Ae = Eu1, Eu2 Ln = Y1 Ln = Y2	Ae = Eu1, Eu2 Ln = Nd2	Ae = Eu3, Eu4 Ln = Nd1	Ae = Eu Ln = Ho	Ae = Ca Ln = Nd Ln = Ho
Ln1–O1	2.120(3)	2.091(3)	2.147(6)	2.086(7)	2.198(4)	2.237(4)
Ln1–O2	2.121(3)	2.102(3)	2.126(6)	2.094(7)	2.205(4)	2.191(4)
Ln1–O3	2.114(3)	2.089(3)	2.112(6)	2.086(7)	2.201(4)	2.209(4)
Ln1–O4	2.083(3)	2.097(3)	2.112(6)	2.122(6)	2.200(4)	2.228(4)
Ae1–O5	2.356(3)	2.446(3)	2.444(6)	2.447(6)	2.420(3)	2.474(4)
Ae1–O6	2.314(3)	2.403(3)	2.433(6)	2.415(7)	2.409(3)	2.445(4)
Ae1–O7	2.332(3)	2.452(3)	2.434(6)	2.474(6)	2.427(3)	2.369(4)
Ae2–O5	2.285(3)	2.463(3)	2.424(6)	2.400(6)	2.441(3)	2.403(4)
Ae2–O6	2.324(3)	2.441(3)	2.474(6)	2.416(7)	2.426(4)	2.403(4)
Ae2–O7	2.327(3)	2.424(3)	2.425(6)	2.475(7)	2.452(3)	2.500(3)
Ae1…Ae2	3.3374(4)	3.5572(3)	3.5762(6)	3.5877(7)	3.5810(4)	3.5561(4)
<b>9</b>	<b>10</b> ·0.5Ph	<b>12</b>	<b>12</b> ·PhMe	<b>12</b> ·4PhMe	<b>13</b>	<b>14</b>
Ae = Ca Ln = Yb	Ae = Sr1, Sr2 Ln = Nd1	Ae = Sr3, Sr4 Ln = Nd2	Ae = Ba Ln = Sm	Ae = Ba Ln = Sm	Ae = Ba Ln = Sm	Ae = Ba Ln = Yb
Ln1–O1	2.064(3)	2.188(9)	2.189(9)	2.171(3)	2.166(3)	2.144(3)
Ln1–O2	2.062(3)	2.194(8)	2.215(9)	2.179(3)	2.149(3)	2.173(3)
Ln1–O3	2.084(3)	2.235(8)	2.20(1)	2.196(3)	2.151(3)	2.163(3)
Ln1–O4	2.068(3)	2.230(8)	2.14(1)	2.185(3)	2.196(3)	2.159(3)
Ae1–O5	2.28(2)	2.440(9)	2.430(8)	2.520(3)	2.608(3)	2.640(3)
Ae1–O6	2.30(2)	2.38(1)	2.477(8)	2.649(3)	2.644(3)	2.575(3)
Ae1–O7	2.33(2)	2.54(1)	2.394(9)	2.683(3)	2.565(3)	2.587(3)
Ae2–O5	2.33(2)	2.422(9)	2.42(1)	2.630(3)	2.608(3)	2.575(3)
Ae2–O6	2.28(2)	2.45(1)	2.397(8)	2.595(3)	2.547(2)	2.621(3)
Ae2–O7	2.29(2)	2.47(1)	2.410(9)	2.544(3)	2.682(3)	2.643(3)
Ae1…Ae2	3.29(3)	3.559(2)	3.546(2)	3.8808(4)	3.9019(7)	3.8857(5)

Table 4. Metal–carbon lengths [Å] for  $\pi$ -Ph–metal interactions in charge-separated heterobimetallic compounds.

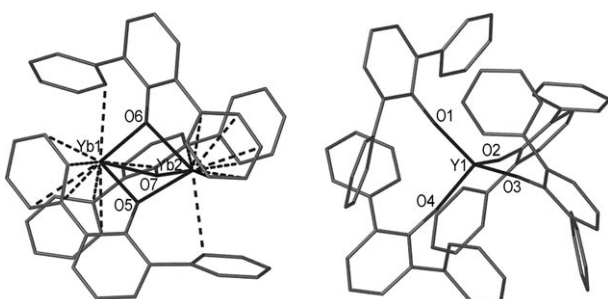
2·2 PhMe	3	3·0.5 PhMe	4	5	6·PhMe	7
Yb1–Cn $\eta^4:\eta^1:\eta^3$	Eu1–Cn $\eta^1:\eta^6:\eta^3$	Eu1–Cn $\eta^3:\eta^6:\eta^1$	Eu3–Cn $\eta^2:\eta^3:\eta^3$	Eu1–Cn $\eta^2:\eta^5:\eta^2$	Eu3–Cn $\eta^4:\eta^3:\eta^1$	Eu1–Cn $\eta^1:\eta^6:\eta^3$
C85 2.887(5)	C80 3.047(5)	C73 3.21(1)	C205 3.11(1)	C79 3.211(5)	C199 3.052(6)	C84 3.058(2)
C86 3.190(5)	C103 3.032(5)	C79 3.03(1)	C206 3.13(1)	C80 2.977(5)	C204 3.233(6)	C103 3.037(2)
C89 3.071(5)	C104 3.074(5)	C80 3.20(1)	C229 3.23(1)	C103 3.077(5)	C211 2.931(6)	C104 3.093(2)
C90 2.826(5)	C105 3.168(5)	C103 2.97(1)	C233 3.26(1)	C104 3.233(7)	C212 3.089(6)	C105 3.179(2)
C102 2.964(5)	C106 3.217(5)	C104 3.05(1)	C234 3.19(1)	C106 3.266(6)	C229 2.990(5)	C106 3.204(2)
C109 3.132(5)	C107 3.175(5)	C105 3.20(1)	C241 3.12(1)	C107 3.100(5)	C230 3.068(5)	C107 3.162(2)
C121 3.038(4)	C108 3.082(5)	C106 3.26(1)	C245 3.24(1)	C108 2.996(5)	C234 3.242(5)	C108 3.071(2)
C126 3.106(5)	C115 3.237(5)	C107 3.21(1)	C246 2.97(1)	C125 3.270(5)	C242 2.953(5)	C115 3.227(3)
				C126 2.967(5)		C119 3.204(2)
						C120 2.913(2)
						C116 3.089(5)
Yb2–Cn $\eta^1:\eta^6:\eta^1$	Eu2–Cn $\eta^4:\eta^2:\eta^1$	Eu2–Cn $\eta^3:\eta^1:\eta^4$	Eu4–Cn $\eta^3:\eta^2:\eta^1$	Eu2–Cn $\eta^3:\eta^2:\eta^2$	Eu4–Cn $\eta^2:\eta^2:\eta^2$	Eu2–Cn $\eta^5:\eta^2:\eta^1$
C80 2.986(4)	C85 2.990(4)	C85 3.16(1)	C211 3.19(1)	C85 3.126(5)	C205 3.184(5)	C85 2.993(2)
C103 2.877(4)	C86 3.034(4)	C89 3.25(1)	C212 3.12(1)	C86 3.183(5)	C210 3.057(6)	C86 3.114(2)
C104 2.960(5)	C87 3.203(5)	C90 3.12(1)	C213 3.21(1)	C90 3.192(5)	C223 3.250(7)	C87 3.277(3)
C105 3.062(5)	C90 3.106(5)	C98 3.01(1)	C223 3.08(1)	C97 3.228(6)	C224 3.122(5)	C89 3.201(2)
C106 3.063(5)	C97 3.217(4)	C115 3.02(1)	C228 3.04(1)	C98 3.137(5)	C247 3.006(7)	C90 3.036(2)
C107 2.979(5)	C98 3.109(4)	C116 3.06(1)	C248 2.98(1)	C115 3.139(5)	C248 3.011(7)	C97 3.210(2)
C108 2.901(5)	C122 3.023(5)	C117 3.27(1)		C116 3.139(5)		C98 3.106(2)
C116 2.864(5)		C120 3.17(1)				C126 3.031(2)
9	10·0.5 PhMe	12	12·PhMe	12·4 PhMe	13	14
Ca1–Cn $\eta^1:\eta^6:\eta^3$	Sr1–Cn $\eta^2:\eta^2:\eta^3$	Sr3–Cn $\eta^5:\eta^1:\eta^2$	Ba1–Cn $\eta^3:\eta^6:\eta^4$	Ba1–Cn $\eta^3:\eta^4:\eta^4$	Ba1–Cn $\eta^3:\eta^4:\eta^4$	Ba1–Cn $\eta^6:\eta^3:\eta^3$
C80 3.06(2)	C79 3.17(1)	C211 3.19(1)	C85 3.331(4)	C79 3.303(4)	C79 3.288(5)	C85 3.215(3)
C103 2.94(2)	C80 3.11(1)	C212 3.26(1)	C86 3.357(4)	C80 3.226(4)	C80 3.209(5)	C86 3.253(3)
C104 2.99(2)	C103 3.25(2)	C214 3.29(2)	C90 3.441(4)	C81 3.354(4)	C81 3.312(5)	C87 3.337(3)
C105 3.04(2)	C104 3.27(2)	C215 3.23(2)	C103 3.229(4)	C97 3.183(4)	C97 3.272(4)	C88 3.357(3)
C106 3.02(2)	C115 3.13(2)	C216 3.18(2)	C104 3.344(5)	C98 3.177(4)	C98 3.281(4)	C89 3.335(3)
C107 2.99(2)	C116 3.02(2)	C224 3.02(1)	C105 3.399(4)	C99 3.415(5)	C99 3.460(4)	C90 3.259(3)
C108 2.95(2)	C117 3.28(2)	C247 3.09(1)	C106 3.365(4)	C102 3.449(4)	C102 3.429(4)	C103 3.409(3)
C109 3.09(2)		C248 3.09(1)	C107 3.292(4)	C115 3.320(4)	C115 3.265(4)	C107 3.462(3)
C115 3.02(2)			C108 3.208(4)	C116 3.456(4)	C116 3.208(4)	C108 3.159(3)
C120 3.07(2)			C121 3.158(4)	C119 3.457(4)	C117 3.344(4)	C121 3.285(3)
			C122 3.425(4)	C120 3.318(4)	C120 3.425(5)	C125 3.260(3)
			C125 3.434(4)			C126 3.077(3)
			C126 3.179(4)			C111 3.412(6)
						C112 3.220(7)
Ca2–Cn $\eta^6:\eta^1:\eta^1$	Sr2–Cn $\eta^4:\eta^2:\eta^1$	Sr4–Cn $\eta^3:\eta^6:\eta^1$	Ba2–Cn $\eta^4:\eta^3:\eta^2$	Ba2–Cn $\eta^4:\eta^6:\eta^4$	Ba2–Cn $\eta^4:\eta^6:\eta^3$	Ba2–Cn $\eta^4:\eta^4:\eta^3$
C85 2.84(2)	C85 3.16(1)	C199 3.23(1)	C73 3.446(4)	C85 3.229(4)	C85 3.259(4)	C79 3.245(3)
C86 2.90(2)	C86 3.27(2)	C205 3.08(2)	C79 3.137(4)	C86 3.338(4)	C86 3.236(4)	C80 3.242(3)
C87 3.06(2)	C89 3.22(2)	C206 3.12(2)	C80 3.195(4)	C89 3.449(4)	C87 3.386(4)	C81 3.441(3)
C88 3.14(2)	C90 3.11(2)	C229 2.99(2)	C84 3.426(4)	C90 3.268(5)	C90 3.429(4)	C84 3.472(3)
C89 3.08(2)	C97 3.07(1)	C230 3.07(2)	C97 3.282(4)	C103 3.287(4)	C103 3.218(4)	C97 3.205(3)
C90 2.92(2)	C98 3.05(1)	C231 3.20(2)	C101 3.390(4)	C104 3.285(4)	C104 3.299(4)	C98 3.314(3)
C102 2.91(2)	C122 2.94(1)	C232 3.26(2)	C102 3.233(4)	C105 3.385(4)	C105 3.409(4)	C101 3.419(3)
C122 2.85(2)		C233 3.19(2)	C115 3.394(4)	C106 3.473(4)	C106 3.437(5)	C102 3.253(3)
		C234 3.06(2)	C120 3.386(4)	C107 3.476(4)	C107 3.362(5)	C115 3.314(3)
		C242 3.10(1)		C108 3.370(4)	C108 3.251(4)	C116 3.222(3)
				C109 3.401(4)	C121 3.261(4)	C117 3.351(3)
				C121 3.160(4)	C125 3.391(4)	
				C122 3.439(4)	C126 3.164(4)	
				C126 3.180(4)		

**Charge-separated complexes  $[(\text{Ln}'/\text{Ae})_2(\text{Odpp})_3][\text{Ln}-(\text{Odpp})_4]$  (1–13) and  $[\text{Ba}_2(\text{Odpp})_3][\text{Mg}(\text{Odpp})_3(\text{thf})]$  (14):** The heterobimetallic complexes **1–14** all feature a charge-separated ion pair, as displayed in the structure of **2·2 PhMe** (Figure 1). The  $[\text{M}_2(\text{Odpp})_3]^+$  cation contains three bridging aryloxide ligands with trigonal-pyramidal geometry around

each metal atom. Except for the  $[\text{Yb}_2(\text{Odpp})_3]^+$  cation in **1·PhMe**,<sup>[11]</sup> all of the few previous examples of the  $[\text{MM}'(\mu-\text{Odpp})_3]$  structural motif have involved two different metals ( $\text{M} \neq \text{M}'$ ) in molecular bimetals (see the Introduction Section). The  $[\text{Ln}(\text{Odpp})_4]^-$  anion consists of four terminal aryloxide ligands arranged around the metal centre in a slightly

Table 5. Metal–carbon lengths [Å] for  $\pi$ -Ph–metal interactions in neutral heterobimetallic compounds.

<b>15</b> ·PhMe	<b>16</b>	<b>16</b> ·PhMe	<b>17</b>	<b>18</b>	<b>18</b> ·PhMe
Ca1–Cn $\eta^6:\eta^1$	Sr1–Cn $\eta^1:\eta^1$	Sr1–Cn $\eta^1:\eta^1:\eta^1$	Ba1–Cn $\eta^2:\eta^1:\eta^1$	Ba1–Cn $\eta^1:\eta^2:\eta^1$	Ba1–Cn $\eta^2:\eta^1:\eta^2$
C221 2.85(1)	C222 3.156(6)	C226 3.22(1)	C221 3.388(6)	C226 3.199(3)	C221 3.351(3)
C222 2.89(1)	C422 3.293(8)	C322 3.09(1)	C226 3.338(6)	C321 3.379(3)	C222 3.329(3)
C223 3.00(1)		C426 3.23(1)	C326 3.285(6)	C326 3.355(3)	C322 3.349(3)
C224 3.10(1)			C426 3.203(6)	C426 3.273(3)	C422 3.246(3)
C225 3.10(1)					C423 3.317(3)
C226 2.98(1)					
C422 3.17(1)					
Eu1–Cn $\eta^2:\eta^3$	Eu1–Cn $\eta^3:\eta^2:\eta^3$	Eu1–Cn $\eta^2:\eta^2:\eta^3$	Sr1–Cn $\eta^3:\eta^5$	Eu1–Cn $\eta^5:\eta^3$	Eu1–Cn $\eta^1:\eta^1:\eta^4$
C161 3.168(4)	C21 3.141(9)	C261 3.021(2)	C361 3.003(6)	C261 3.052(3)	C262 3.112(3)
C162 3.022(4)	C261 3.045(9)	C262 3.107(2)	C362 3.285(6)	C262 3.146(3)	C361 3.015(3)
C261 2.998(3)	C262 3.236(9)	C361 3.027(2)	C366 3.223(6)	C263 3.277(3)	C461 3.020(3)
C265 3.050(4)	C361 3.091(9)	C362 3.006(2)	C461 3.084(6)	C265 3.241(4)	C462 3.187(3)
C266 2.839(4)	C366 3.155(9)	C41 3.261(2)	C462 3.122(6)	C266 3.097(3)	C465 3.181(3)
	C461 3.035(9)	C461 2.991(2)	C463 3.257(6)	C461 3.010(3)	C466 3.007(3)
	C462 3.125(8)	C466 3.171(2)	C465 3.270(7)	C462 3.209(3)	
	C466 3.184(9)		C466 3.164(6)	C466 3.292(3)	

Figure 1. Structure of  $[Yb_2(Odpp)_3][Y(Odpp)_4] \cdot 2\text{PhMe}$ , **2**·0.5PhMe. Hydrogen atoms and toluene molecules of solvation are omitted for clarity.

distorted tetrahedral geometry. No  $\pi$ -Ph–metal interactions are evident in the anion because the substantial steric bulk of four aryloxide ligands sufficiently shields the metal centre despite the low coordination number. The  $[\text{Ln}(\text{Odpp})_4]^-$  anion has been previously observed in the structures of **1**·PhMe,<sup>[11]</sup>  $[\text{Na}(\text{Nd}(\text{Odpp}))_4]$ ,<sup>[26,27]</sup>  $[\text{K}(\text{Ln}(\text{Odpp}))]$  ( $\text{Ln} = \text{La}, \text{Nd}$ ),<sup>[28]</sup>  $[\text{Na}(\text{dme})_3][\text{Nd}(\text{Odpp})_4]$ <sup>[27]</sup> and  $[\text{Na}(\text{dig})_2][\text{Ln}(\text{Odpp})_4]$  ( $\text{Ln} = \text{Nd}, \text{Er}$ ),<sup>[27]</sup> a quite limited collection.

Although the structure of the  $[(\text{Ln}'/\text{Ae})(\text{Odpp})_3]^+$  cations in **1–14** appear to be similar, there are some notable differences. The structures display variations in the magnitude of the  $\pi$ -Ph–metal interactions. These are not entirely due to differences in the ionic radii of the metal because slight variations are also evident between different structures that contain the same cation, and are associated with differences in the orientation of the aryloxides and pendant phenyl groups relative to the metal atoms. The slight differences in the cations, which in turn affect the packing of the molecules in the crystal structure, may account for the wide range of unit cell dimensions observed for **1–14** (see the Experimental Section herein and Table S1 and the Experi-

mental Section in the Supporting Information). For brevity the complexes are discussed in groups containing the same cation.

**Structures containing a  $[Yb_2(Odpp)_3]^+$  cation:** Compounds **1a** and **1b** both contain two crystallographically independent  $[Yb_2(\text{Odpp})_3]^+$  cations and  $[\text{Yb}(\text{Odpp})_4]^-$  anions in the asymmetric unit, but the unit cell dimensions are different (see the Supporting Information Experimental Section). Otherwise, **1a** and **1b** are comparable to  $[Yb_2(\text{Odpp})_3][\text{Yb}(\text{Odpp})_4]\cdot\text{PhMe}$  (**1**·PhMe).<sup>[16]</sup> The crystal structure of **2**·0.5PhMe revealed two similar but crystallographically independent  $[Yb_2(\text{Odpp})_3]^+$  cations and  $[\text{Yb}(\text{Odpp})_4]^-$  anions and also toluene of solvation. Both anion–metal positions in **2**·0.5PhMe were found to be disordered Y/Yb approximately 70:30. Disorder in the metal positions of heterobimetallic complexes containing the Odpp ligand has previously been observed in the structures of  $[\text{KBa}(\text{Odpp})_3]\cdot\text{PhMe}$ <sup>[14]</sup> and  $[\text{KSr}(\text{Odpp})_3]\cdot\text{PhMe}$ ,<sup>[15]</sup> in which the metal positions were disordered K/Ba and K/Sr 50:50. The crystal structures of **2**·1.5PhMe and **2**·2PhMe contain a  $[Yb_2(\text{Odpp})_3][\text{Yb}(\text{Odpp})_4]$  molecule and one-and-a-half or two toluene molecules of solvation and have no metal position disorder. In the cation of **2**·2PhMe, Yb–O bond lengths (2.285(3)–2.356(3) Å) result in a Yb···Yb separation of 3.337(1) Å. These bond lengths and the Yb···Yb separation are comparable with the analogous lengths in the structure of **1**·PhMe,<sup>[11]</sup> (2.289(7)–2.327(7) Å for Yb–O and 3.348(1) Å for Yb···Yb). In the  $[Yb_2(\text{Odpp})_3]^+$  cation of **2**·2PhMe, Yb1 has  $\eta^4:\eta^1:\eta^3$ -Ph–Yb interactions (Yb–C 2.83(1)–3.19(1) Å) whereas Yb2 displays  $\eta^1:\eta^6:\eta^1$  interactions (Yb–C 2.86(1)–3.06(1) Å). In the  $[Yb_2(\text{Odpp})_3]^+$  cation of **1**·PhMe, the two metals exhibit  $\eta^6:\eta^1:\eta^1$  and  $\eta^6:\eta^2:\eta^1$  interactions<sup>[11]</sup> with Yb–C interactions (2.85(1)–3.15(1) Å) comparable to those of **2**·2PhMe. The longest Yb–C length in **2**·2PhMe that is classified as bonding (3.19(1) Å) is close to the maximum bonding length in **1**·PhMe (3.15(1) Å) and is also similar to the maximum  $\pi$ -Ph–Yb interaction distance in the structure of  $[\text{Yb}^{III}(\text{Odpp})_3]$  (3.15(1) Å),<sup>[29]</sup> despite the approximately 0.15 Å larger ionic radius of  $\text{Yb}^{2+}$  compared with  $\text{Yb}^{3+}$  (for the same coordination number).<sup>[21]</sup> Considering the approximately 0.04 Å larger ionic radius of  $\text{Yb}^{2+}$  than  $\text{Nd}^{3+}$ , the maximum  $\pi$ -Ph–Yb interaction distance of 3.19(1) Å in **2**·2PhMe is comparable with the maximum  $\pi$ -Ph–Nd interaction distance of 3.18(1) in the structure of  $[[\text{Nd}(\text{OAr}^2)_2(\mu-\{\text{O}:\eta^6-\text{Ar}^2\}-\text{OAr}^2)]_2]$ .<sup>[30]</sup> In the cation of **2**·2PhMe there are a wide range of Yb–O–C angles (Table S2 in the

Supporting Information), but there often appears to be a correlation between the hapticity of the  $\pi$ -Ph–Yb interactions and the angle; for example, aryloxide ligand O6 is bound  $\eta^1$  to Yb1 and  $\eta^6$  to Yb2, and the Yb1–O6–C91 angle is 138.0(3) $^\circ$  whereas the Yb2–O6–C91 angle is 129.9(3) $^\circ$ . The greater tilt towards Yb2 presumably relates to the more substantial  $\pi$ -Ph–Yb interaction with Yb2.

The X-ray data unequivocally show that the metal position in the anion in **2**·2PhMe contains  $\text{Y}^{3+}$  rather than  $\text{Yb}^{3+}$ . The average Yb–O bond length in the  $[\text{Yb}(\text{Odpp})_4]^-$  anion of **1**·PhMe is 2.07 Å, whereas for **2**·2PhMe the average Y–O bond length is 2.11 Å. Subtraction of the four-coordinate ionic radius of the  $\text{Ln}^{3+}$  ion (extrapolated from Shannon's data)<sup>[16]</sup> from the average Ln–O bond length of  $[\text{Ln}(\text{Odpp})_4]^-$  gives 1.31 Å for  $\text{Yb}^{3+}$  in **1**·PhMe and 1.33 Å for  $\text{Y}^{3+}$  in **2**·2PhMe.

*Structures containing a  $[\text{Eu}_2(\text{Odpp})_3]^+$  cation:* The  $[\text{Eu}_2(\text{Odpp})_3]^+$  cations in the structures of **3** (Figure 2), **3**·0.5PhMe, **4** and **5** are very similar and consequently have

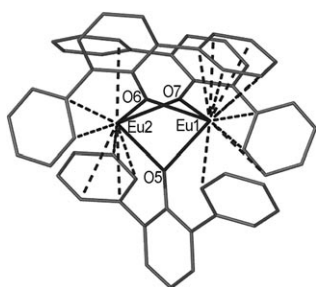


Figure 2. Structure of the  $[\text{Eu}_2(\text{Odpp})_3]^+$  cation in  $[\text{Eu}_2(\text{Odpp})_3](\text{Y}(\text{Odpp})_4)$ , **3**. Hydrogen atoms are omitted for clarity.

comparable bond lengths (Table 2). The fundamental structural framework of the cations in these structures is similar to that of  $[\text{Yb}_2(\text{Odpp})_3]^+$ . The structure of **3** consists of a  $[\text{Eu}_2(\text{Odpp})_3]^+$  cation (Figure 2) and a  $[\text{Y}(\text{Odpp})_4]^-$  anion. In **3**·0.5PhMe, two similar but crystallographically independent cations and anions and a molecule of toluene are present in the asymmetric unit. In addition to the  $[\text{Eu}_2(\text{Odpp})_3]^+$  cation, the structures of **4** and **5** contain  $[\text{Nd}(\text{Odpp})_4]^-$  and  $[\text{Ho}(\text{Odpp})_4]^-$  anions, respectively, with the structure of **4** having two crystallographically independent  $[\text{Eu}_2(\text{Odpp})_3]^+$  cations and  $[\text{Nd}(\text{Odpp})_4]^-$  anions in the asymmetric unit. Only the representative  $[\text{Eu}_2(\text{Odpp})_3]^+$  cation in **3** is discussed in detail, but the cation in **4**, which displays the greatest variation in Eu–O bond lengths, is also briefly considered.

In the structure of **3**, Eu–O bond lengths in the cation range from 2.403(1) to 2.463(1) Å (average 2.44 Å), which is in good agreement with the Yb–O bond lengths in the  $[\text{Yb}_2(\text{Odpp})_3]^+$  cations after allowing for the 0.15 Å difference in ionic radii between  $\text{Eu}^{2+}$  and  $\text{Yb}^{2+}$ .<sup>[16]</sup> As with the  $[\text{Yb}_2(\text{Odpp})_3]^+$  cations, the narrow range of Eu–O bond lengths in **3** indicates near-symmetrical bridging of the aryloxide

ligand between the two europium metal atoms. This contrasts with the wider range of Eu–O(bridging) bond lengths in  $[\text{Eu}_2(\text{Odpp})_4]\cdot\text{PhMe}$  (2.426(8)–2.517(3) Å),<sup>[11]</sup> in which there is a terminal aryloxide ligand on Eu1 and a difference in coordination number between the two Eu atoms. The Eu–O–Eu and O–Eu1,2–O angles (see the Supporting Information) resemble the corresponding angles in the  $[\text{Yb}_2(\text{Odpp})_3]^+$  cations, which indicates a similar ligand arrangement around the lanthanoid metals in the two cations.

In the structure of **3**, the  $\pi$ -Ph–Ln interactions are similar to those observed in  $[\text{Yb}_2(\text{Odpp})_3]^+$  cations (see Table 4). Eu1 is bound in a  $\eta^1:\eta^6:\eta^3$  fashion, whereas Eu2 has  $\eta^4:\eta^2:\eta^1$  interactions. The  $\pi$ -Ph–Eu contacts range from 2.910(4) to 3.237(5) Å and agree well with the range of  $\pi$ -Ph–Eu interactions in  $[\text{Eu}_2(\text{Odpp})_4]\cdot\text{PhMe}$  (2.987(4)–3.240(4) Å).<sup>[11]</sup> Despite the larger size of  $\text{Eu}^{2+}$  compared with  $\text{Yb}^{2+}$ , shielding of the naked faces does not involve significantly enhanced  $\pi$ -bonding. This contrasts with  $[\text{Ba}_2(\text{Odpp})_4]$ <sup>[17]</sup> and  $[\text{Eu}_2(\text{Odpp})_4]\cdot\text{PhMe}$ <sup>[11]</sup> in which similar structural frameworks have more extensive  $\pi$ -Ph–metal interactions for the larger Ba atoms. Similarly, in the three  $[\text{M}(\text{Nd}(\text{Odpp})_4)]$ ,<sup>[26–28]</sup>  $[\text{MAe}(\text{Odpp})_3]$  and  $[\text{Li}_2\text{Ae}(\text{Odpp})_4]$ <sup>[14,15]</sup> ( $\text{M}=\text{Na}, \text{K}; \text{Ae}=\text{Ca}, \text{Sr}, \text{Ba}$ ) series, different  $\pi$ -Ph–metal interactions were observed for different metals with the same structural framework. In cation 2 (Eu3 and Eu4) of **4**, there is a significant difference in the Eu–O14 bond lengths (Eu3–O14 2.369(4) Å, Eu4–O14 2.500(3) Å), with both being outside the Eu–O range of **3**. This asymmetric binding mode is unexpected given that pendant phenyl groups on the O14 ligand bind only  $\eta^1$  to Eu3 and  $\eta^2$  to Eu4. Nevertheless, the O14 ligand is markedly tilted towards Eu4 (Eu3–O14–C235 143.8(3) $^\circ$ ; Eu4–O14–C235 119.6(3) $^\circ$ ). Thus the variation in Eu–O14 bond length is likely to be a result of enhanced steric crowding around Eu4.

The  $[\text{Y}(\text{Odpp})_4]^-$  anions in **3** and **3**·0.5PhMe are very similar and the bond lengths and angles around the Y metal atom are in agreement with the same anion of **2**·2PhMe. The  $[\text{Nd}(\text{Odpp})_4]^-$  and  $[\text{Ho}(\text{Odpp})_4]^-$  anions in the structures of **4** and **5**, respectively, also display slightly distorted tetrahedral geometry around the metal atom with, as expected, different Ln–O bond lengths (averages 2.096 Å for  $[\text{Ho}(\text{Odpp})_4]^-$ ; 2.201 Å (anion 1) and 2.216 Å (anion 2) for  $[\text{Nd}(\text{Odpp})_4]^-$ ). Subtraction of the four-coordinate ionic radius of the  $\text{Ln}^{3+}$  ion (extrapolated)<sup>[16]</sup> from the Ln–O bond lengths in  $[\text{Ln}(\text{Odpp})_4]^-$  gives 1.31 Å for **5** and 1.34 and 1.36 Å for anion 1 and anion 2, respectively, of **4**.

*Structures containing a  $[\text{Ca}_2(\text{Odpp})_3]^+$  cation:* The  $[\text{Ca}_2(\text{Odpp})_3]^+$  cations in the crystal structures of **6**·PhMe, **7** and **9** are very similar, as seen from the pertinent bond lengths listed in Table 2. Consequently, only the structure of the cation of **6**·PhMe is discussed in detail. In the structure of **9**, both metal positions in the cation are disordered Ca/Yb 70:30, which perhaps arises from the similarities in ion size, but the anion is not disordered. The bond lengths in the cation of **6**·PhMe correlate quite well with the analogous values in  $[\text{Yb}_2(\text{Odpp})_3]^+$  cations (Table 3), further reflecting

the similar ionic radii of  $\text{Ca}^{2+}$  and  $\text{Yb}^{2+}$ .<sup>[16]</sup> The  $\text{Ca1}-\text{O}$  and  $\text{Ca2}-\text{O}$  bond lengths (2.269(3)–2.293(3) Å; 2.258(3)–2.267(3) Å) indicate near symmetric binding of the aryloxide ligands and are similar to bridging  $\text{Ca}-\text{O}$  bond lengths (2.249(2)–2.275(2) Å) in the structure of  $[\text{Ca}_2(\text{Odpp})_4]\cdot\text{PhMe}$ .<sup>[17]</sup> A smaller  $\text{Ca}\cdots\text{Ca}$  length in the cation of **6**·PhMe (3.231(2) Å) than in  $[\text{Ca}_2(\text{Odpp})_4]\cdot\text{PhMe}$  (3.582(1) Å) is most likely due to the additional bridging aryloxide ligand in **6**·PhMe. The  $\text{Yb}\cdots\text{Yb}$  lengths in  $[\text{Yb}_2(\text{Odpp})_4]\cdot1.5\text{PhMe}$  and **1**·PhMe show a similar trend.<sup>[11]</sup>

The shrouding pendant phenyl groups bind  $\eta^1:\eta^2:\eta^6$  to  $\text{Ca1}$  and  $\eta^1:\eta^1:\eta^6$  to  $\text{Ca2}$ .  $\text{Ca}-\text{C}$  interaction distances range from 2.871(5) to 3.176(6) Å, with the upper value agreeing well with that for  $\pi\text{-Ph-Yb}$  bonding in **2**·2PhMe (3.190(5) Å). The donor hapticities of **6**·PhMe and **1**·PhMe are the same and their unit cell dimensions are similar, which is consistent with the above suggestion that the large number of different unit cell dimensions observed for the  $[(\text{Ln}'/\text{Ae})_2(\text{Odpp})_3][\text{Ln}(\text{Odpp})_4]$  complexes may be linked to differences in  $\pi\text{-Ph-met}$  interactions. The similarities between the  $\pi\text{-Ph-met}$  interactions of **6**·PhMe and **1**·PhMe contrast with the differences in  $\pi\text{-Ph-met}$  interactions between structurally similar  $[\text{Ca}_2(\text{Odpp})_4]\cdot\text{PhMe}$  ( $\eta^1:\eta^3$  and  $\eta^6$ )<sup>[17]</sup> and  $[\text{Yb}_2(\text{Odpp})_4]\cdot1.5\text{PhMe}$  ( $\eta^4:\eta^3$  and  $\eta^1:\eta^6$ ).<sup>[11]</sup> Enhanced  $\pi$ -bonding in  $[\text{Ca}_2(\text{Odpp})_3]^+$  compared with  $[\text{Ca}_2(\text{Odpp})_4]\cdot\text{PhMe}$  can be attributed to the absence of terminal ligands in the former as well as the cationic nature.

The average  $\text{Ln}-\text{O}$  bond lengths in the  $[\text{Nd}(\text{Odpp})_4]^-$  (2.208 Å),  $[\text{Ho}(\text{Odpp})_4]^-$  (2.106 Å) and  $[\text{Yb}(\text{Odpp})_4]^-$  (2.070 Å) anions of **6**·PhMe, **7** and **9**, respectively, compare well with the previously discussed  $[\text{Ln}(\text{Odpp})_4]^-$  anions. Subtraction of the ionic radius of the relevant four-coordinate  $\text{Ln}^{3+}$  ion (extrapolated)<sup>[16]</sup> from the average  $\text{Ln}-\text{O}$  bond lengths in the  $[\text{Ln}(\text{Odpp})_4]^-$  anion gives lengths of 1.35, 1.32 and 1.32 Å for the anions in **6**·PhMe, **7** and **8**, respectively.

**Structures containing a  $[\text{Sr}_2(\text{Odpp})_3]^+$  cation:** The crystal structure of **10**·0.5PhMe revealed two similar but crystallographically independent  $[\text{Sr}_2(\text{Odpp})_3]^+$  cations and  $[\text{Nd}(\text{Odpp})_4]^-$  anions and one toluene molecule in the lattice. The  $\text{Ho}^{3+}$  analogue, **11**·0.5PhMe, is isomorphous. The  $\text{Sr}-\text{O}$  bond lengths in the  $[\text{Sr}_2(\text{Odpp})_3]^+$  cations of **10**·0.5PhMe range from 2.38(1) to 2.54(1) Å (average 2.45 Å) for cation 1 ( $\text{Sr1}$  and  $\text{Sr2}$ ) and 2.394(9) to 2.477(8) Å (average 2.42 Å) for cation 2 ( $\text{Sr3}$  and  $\text{Sr4}$ ). Due to the comparable ionic radii of  $\text{Sr}^{2+}$  and  $\text{Eu}^{2+}$ ,<sup>[16]</sup> the average  $\text{Sr}-\text{O}$  bond lengths correlate well with the average  $\text{Eu}-\text{O}$  bond length (2.44 Å) in **3**, although the bond length range for **10**·0.5PhMe is wider than for **3**. In the structure of  $[\text{Sr}_2(\text{Odpp})_4]\cdot\text{PhMe}$ ,<sup>[17]</sup> which contains three bridging ligands and one terminal ligand, the  $\text{Sr}-\text{O}$  bond lengths (2.430(2)–2.499(2) Å) for the bridging aryloxides are close to the analogous values for **10**·0.5PhMe.

In **10**·0.5PhMe,  $\pi\text{-Ph-Sr}$  interactions are  $\eta^2:\eta^2:\eta^3$  for  $\text{Sr1}$ ,  $\eta^4:\eta^2:\eta^1$  for  $\text{Sr2}$  (cation 1, Figure 3),  $\eta^5:\eta^2:\eta^1\text{-Ph-Sr}$  for  $\text{Sr3}$  and  $\eta^3:\eta^6:\eta^1$  for  $\text{Sr4}$  (cation 2). The  $\text{Sr}-\text{C}$  lengths range from 2.94(1) to 3.28(2) Å and 2.99(1) to 3.29(2) Å for the respec-

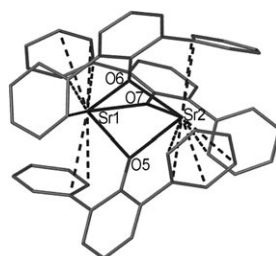


Figure 3. Structure of the  $[\text{Sr}_2(\text{Odpp})_3]^+$  cation (cation 1) in  $[\text{Sr}_2(\text{Odpp})_3][\text{Nd}(\text{Odpp})_4]\cdot0.5\text{PhMe}$  (**10**·0.5PhMe). Hydrogen atoms and toluene molecule of solvation are omitted for clarity.

tive cations. These differences may explain the smaller  $\text{Sr}-\text{O}$  bond length range and shorter  $\text{Sr}\cdots\text{Sr}$  length for cation 2 compared with cation 1. Cation 2 has very similar  $\pi\text{-Ph-met}$  interactions to **3** whereas cation 1 has lower hapticity; this is another example showing the flexibility of  $\pi\text{-Ph-met}$  interactions. Due to the absence of terminal ligands, the  $[\text{Sr}_2(\text{Odpp})_3]^+$  cations in **10**·0.5PhMe display more extensive  $\pi\text{-Ph-Sr}$  interactions than the structure of  $[\text{Sr}_2(\text{Odpp})_4]\cdot\text{PhMe}$  ( $\eta^1:\eta^1:\eta^1$ ) at  $\text{Sr1}$  and ( $\eta^2:\eta^2:\eta^2$ ) at  $\text{Sr2}$ .<sup>[17]</sup> The  $\text{Sr}-\text{C}$  bond lengths in **10**·0.5PhMe are slightly longer than those in  $[\text{Sr}_2(\text{Odpp})_4]\cdot\text{PhMe}$ , but are in good agreement with the  $\text{Sr}-\text{C}$  lengths in the structure of  $[\text{NaSr}(\text{Odpp})_3]\cdot\text{PhMe}$  (3.051(2)–3.310(3)).<sup>[15]</sup> In **10**·0.5PhMe the angle  $\text{Sr4-O12-C199}$  (115.7(8)°) is much smaller than  $\text{Sr3-O12-C199}$  (139.3(9)°), which indicates that the ligand is tilted towards  $\text{Sr4}$ . However, the  $\text{Sr3}-\text{O12}$  and  $\text{Sr4}-\text{O12}$  bond lengths are comparable and, surprisingly, ligand O12 displays more extensive  $\pi\text{-Ph-Sr}$  interactions with  $\text{Sr3}$  than with  $\text{Sr4}$  ( $\eta^5$  vs.  $\eta^3$ ). The tilting of ligand O12 towards  $\text{Sr4}$  may permit the two pendant phenyl groups of ligand O12 to adopt the most favourable positions for optimising  $\pi\text{-Ph-Sr}$  interactions with *both* metals. The average  $\text{Nd}-\text{O}$  bond lengths of the  $[\text{Nd}(\text{Odpp})_4]^-$  anions in **10**·0.5PhMe are comparable with those of  $[\text{Nd}(\text{Odpp})_4]^-$  in **4** and **6**·PhMe.

**Structures containing a  $[\text{Ba}_2(\text{Odpp})_3]^+$  cation:** The  $[\text{Ba}_2(\text{Odpp})_3]^+$  cations in the crystal structures of **12**, **12**·PhMe, **12**·4PhMe, **13** and **14** (Figure 4) are very similar, as seen from the pertinent bond lengths listed in Table 2. The anion in the crystal structures of **12**, **12**·PhMe and **12**·4PhMe is

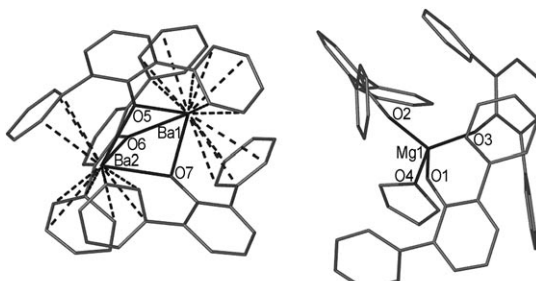


Figure 4. Structure of  $[\text{Ba}_2(\text{Odpp})_3][\text{Mg}(\text{Odpp})_3(\text{thf})]$  (**14**). Hydrogen atoms are omitted for clarity.

[Sm(Odpp)<sub>4</sub>]<sup>-</sup>, which has not been previously represented in the charge-separated complexes, whereas the anions in **13** and **14** are [Yb(Odpp)<sub>4</sub>]<sup>-</sup> and [Mg(Odpp)<sub>3</sub>(thf)]<sup>-</sup>, respectively. Ba–O bond lengths in **12**·PhMe, **13** and **14** fall within a narrow range (2.556(2)–2.682(3) Å, Table 2) and are comparable with those in [M[Ba(Odpp)<sub>3</sub>]] (M=Na, K, Cs).<sup>[14]</sup> In [Ba<sub>2</sub>(Odpp)<sub>4</sub>]<sup>[17]</sup> the Ba–O bond lengths (2.506(2)–2.887(2) Å) for the bridging ligands have a larger range, perhaps owing to the presence of a terminal Odpp ligand on Ba1. The trigonal-pyramidal arrangement and more symmetrical bridging of the metal atoms in the [Ba<sub>2</sub>(Odpp)<sub>3</sub>]<sup>+</sup> cation is characterised by a narrower range of O–Ba–O (68.18(8)–71.68(9)°) and Ba–O–Ba (94.72(6)–98.1(1)°) angles in **12**·PhMe, **13** and **14** than in [Ba<sub>2</sub>(Odpp)<sub>4</sub>] (O–Ba–O: 66.01(7)–76.99(7)°; Ba–O–Ba: 92.65(7)–98.31(8)°).<sup>[17]</sup>

The Ba···Ba lengths in **12**·PhMe, **13** and **14** (3.902(1), 3.865(1) and 3.898(1) Å, respectively) are marginally shorter than in [Ba<sub>2</sub>(Odpp)<sub>4</sub>] (3.928(1) Å), which is attributable to differences in π-Ph–Ba interactions between the two structures. An opposite trend was observed when comparing the Eu···Eu and Sr···Sr lengths in the [Eu<sub>2</sub>(Odpp)<sub>3</sub>]<sup>+</sup> cation of **3** and the [Sr<sub>2</sub>(Odpp)<sub>3</sub>]<sup>+</sup> cation of **10**·0.5PhMe with those of [Eu<sub>2</sub>(Odpp)<sub>4</sub>]·PhMe<sup>[11]</sup> and [Sr<sub>2</sub>(Odpp)<sub>4</sub>]·PhMe,<sup>[17]</sup> respectively. This suggests that although the gross features of the [Eu<sub>2</sub>(Odpp)<sub>3</sub>]<sup>+</sup>, [Sr<sub>2</sub>(Odpp)<sub>3</sub>]<sup>+</sup> and [Ba<sub>2</sub>(Odpp)<sub>3</sub>]<sup>+</sup> cations appear to be similar, the larger ionic radius of Ba<sup>2+</sup> compared with Eu<sup>2+</sup> and Sr<sup>2+</sup> gives rise to structural differences.

In the [Ba<sub>2</sub>(Odpp)<sub>3</sub>]<sup>+</sup> cations of **12**, there are η<sup>3</sup>-Ph–Ba, η<sup>4</sup>-Ph–Ba and η<sup>6</sup>-Ph–Ba interactions at Ba1, whereas at Ba2 there are η<sup>4</sup>-Ph–Ba, η<sup>2</sup>-Ph–Ba and η<sup>3</sup>-Ph–Ba interactions. The Ba–C lengths (3.137(4)–3.446(4) Å) are in agreement with the Ba–C bond lengths in [Ba<sub>2</sub>(Odpp)<sub>4</sub>] (3.075(3)–3.449(4) Å).<sup>[17]</sup> The slightly different π-Ph–Ba interactions evident in the [Ba<sub>2</sub>(Odpp)<sub>3</sub>]<sup>+</sup> cations of **12**·PhMe, **12**·4PhMe, **13** and **14** (Table 4) may be rationalised by differences in orientation of the phenyl substituents, which are possibly induced by solvation or the differences in the counterions. Due to the absence of terminal ligands, the [Ba<sub>2</sub>(Odpp)<sub>3</sub>]<sup>+</sup> cations display more extensive π-Ph–Ba interactions than [Ba<sub>2</sub>(Odpp)<sub>4</sub>] (η<sup>1</sup>:η<sup>1</sup>:η<sup>2</sup> at Ba1 and η<sup>3</sup>:η<sup>6</sup>:η<sup>2</sup> at Ba2).<sup>[17]</sup> Furthermore, the π-Ph–Ba interactions in the [Ba<sub>2</sub>(Odpp)<sub>3</sub>]<sup>+</sup> cations are more extensive than in the analogous [M<sub>2</sub>(Odpp)<sub>3</sub>]<sup>+</sup> (M=Yb, Eu, Ca, Sr) cations, which reflects the larger size of Ba<sup>2+</sup>.

The Sm–O lengths in the [Sm(Odpp)<sub>4</sub>]<sup>-</sup> anion of **12**·PhMe range from 2.149(3) to 2.196(3) Å with an average of 2.17 Å. After adjusting for the differences in the ionic radii of the four-coordinate Ln<sup>3+</sup> ion,<sup>[16]</sup> the Sm–O bond lengths in the anion of **12**·PhMe are in good agreement with the Yb–O bond lengths in the anion of **1**·PhMe (2.053(6)–2.094(7) Å),<sup>[11]</sup> as are the Yb–O bond lengths in **13** (2.052(2)–2.071(2) Å). There are very few tetra-coordinated magnesium alkoxides or aryloxides that can be compared to the [Mg(Odpp)<sub>3</sub>(thf)] anion in **14** (Figure 4). Most are neutral with two aryloxide moieties and either two neutral donor ligands, as in [Mg(Odpp)<sub>2</sub>(thf)<sub>2</sub>],<sup>[25]</sup> [Mg(Et<sub>2</sub>O)<sub>2</sub>(Odpp)<sub>2</sub>],<sup>[25]</sup> and [Mg(OAr<sup>3</sup>)<sub>2</sub>(thf)<sub>2</sub>] (OAr<sup>3</sup>=2,6-di-*tert*-butyl-

phenolate),<sup>[31]</sup> or a bidentate donor, as in [Mg(OAr<sup>3</sup>)<sub>2</sub>(tmEDA)] (tmEDA=N,N,N',N'-tetramethylmethylenediamine).<sup>[31]</sup> The most closely related unassociated magnesiate species is the triangular planar three-coordinate [Mg(OAr<sup>4</sup>)<sub>3</sub>]<sup>-</sup> (OAr<sup>4</sup>=2,6-di-*tert*-butyl-4-methylphenolate).<sup>[25]</sup> The enhanced steric demand of this ligand is indicated by the isolation of an unsolvated complex in the presence of thf compared with the isolation of thf-complexed **14**. The Mg–Odpp bond lengths in **14** (1.869(4)–1.892(4) Å) are somewhat longer than those in [Mg(OAr<sup>4</sup>)<sub>3</sub>]<sup>-</sup> (1.839(1)–1.848(1) Å),<sup>[25]</sup> in accordance with the coordination number difference. The Mg–Odpp and Mg–O(thf) bond lengths in **14** (average 1.88 and 2.04 Å, respectively) are comparable with those in [Mg(Odpp)<sub>2</sub>(thf)<sub>2</sub>] (average 1.88 and 2.03 Å) and [Mg(Odpp)<sub>2</sub>(Et<sub>2</sub>O)<sub>2</sub>] (average 1.88 and 2.04 Å).<sup>[25]</sup>

### Neutral dinuclear complexes [AeEu(Odpp)<sub>4</sub>] and [BaSr(Odpp)<sub>4</sub>]

*The structure of [CaEu(Odpp)<sub>4</sub>] (**15**):* The structure of **15**·PhMe (Figure 5) revealed a heterodinuclear complex with two aryloxide ligands bridging the Ca<sup>2+</sup> and Eu<sup>2+</sup>

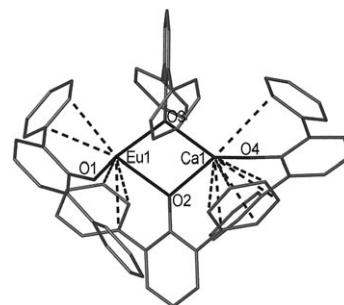


Figure 5. Structure of [CaEu(Odpp)<sub>4</sub>]·PhMe (**15**·PhMe). Hydrogen atoms and toluene molecule of solvation are omitted for clarity.

metal atoms and a terminal aryloxide ligand on each. Both metals are three (oxygen) coordinate. The basic metal–oxygen framework of **15**·PhMe resembles the structure of [Ca<sub>2</sub>(Odpp)<sub>4</sub>]·PhMe,<sup>[17]</sup> an observation supported by the comparable unit cell dimensions of the two structures. Note that the [Ca<sub>2</sub>(Odpp)<sub>4</sub>]·PhMe structural motif of the smaller metal is adopted, rather than that of [Eu<sub>2</sub>(Odpp)<sub>4</sub>]·PhMe, which has three bridging aryloxide ligands.<sup>[11]</sup> The metal positions in **15**·PhMe are disordered (Eu1: Eu/Ca 55:45; Ca2: Ca/Eu 70:30), giving a slight excess of Ca (Ca/Eu 1.14:0.86), and this may dictate adoption of the [Ca<sub>2</sub>(Odpp)<sub>4</sub>] framework. X-ray data were collected on several crystals and all were similarly disordered.

The Eu–O(bridging) aryloxide bond lengths are 2.368(3) and 2.491(3) Å (average 2.43 Å), whereas the Eu–O bond length for the terminal ligand is 2.303(3) Å (Table 3). In the structure of [Eu<sub>2</sub>(Odpp)<sub>4</sub>]·PhMe<sup>[11]</sup> the average Eu–O(bridging) bond length is longer (2.48 Å), as is the terminal Eu–O bond (2.361(3) Å), due to the presence of three bridging ligands rather than two in **15**·PhMe. The Ca–O-

(bridging) aryloxide bond lengths in **15**·PhMe (2.28(1) and 2.30(1) Å) are comparable with those of  $[\text{Ca}_2(\text{Odpp})_4]\cdot\text{PhMe}$  (2.275(2), 2.249(2) Å).<sup>[17]</sup> Likewise, the Ca–O bond lengths for the terminal ligands (2.118(9) vs. 2.122(2) Å) are similar, as are the O–Ca–O angles for the bridging aryloxide ligands (75.5(3) vs. 75.3(1)°).

The voids in the metal coordination spheres owing to the distorted trigonal-pyramidal geometry around the  $\text{Ca}^{2+}$  and  $\text{Eu}^{2+}$  ions in **15**·PhMe are occupied by pendant phenyl groups, resulting in  $\pi$ -Ph–metal interactions that provide coordinative saturation. Eu1 has  $\eta^2$ -Ph and  $\eta^3$ -Ph interactions (Eu–C 2.839(4)–3.168(4) Å), whereas Ca1 has  $\eta^6$ -Ph and  $\eta^1$ -Ph interactions (Ca–C 2.85(1)–3.17(1) Å; Table 5). As in the structure of  $[\text{Ca}_2(\text{Odpp})_4]\cdot\text{PhMe}$ ,<sup>[17]</sup> only one bridging aryloxide ligand contributes to the  $\pi$ -Ph–metal interactions. The  $\eta^1$  contact involves the terminal Odpp ligand. For Eu1, the  $\pi$ -Ph–Eu interactions differ from those of the Eu atoms of  $[\text{Eu}_2(\text{Odpp})_4]\cdot\text{PhMe}$ <sup>[11]</sup> ( $\eta^3:\eta^3:\eta^3$  or  $\eta^1:\eta^1:\eta^1$ ; Eu–C 2.987(4)–3.240(4) Å), reflecting the differences in the coordination environments. However, for Ca1 in **15**·PhMe the  $\eta^6$ -Ph and  $\eta^1$ -Ph interactions resemble the  $\pi$ -Ph–Ca interactions of Ca2 in  $[\text{Ca}_2(\text{Odpp})_4]\cdot\text{PhMe}$ ,<sup>[17]</sup> both in the hapticity of the interactions and in the Ca–C lengths (2.862(2)–3.158(3) Å).

**The structure of  $[\text{SrEu}(\text{Odpp})_4]$  (16):** Compounds **16** and **16**·PhMe display an unsymmetrical dinuclear structure with three aryloxide ligands bridging  $\text{Sr}^{2+}$  and  $\text{Eu}^{2+}$  and a terminal aryloxide ligand bound to Sr1. Because of common structural features, only the structure of **16** (similar to that of **18** in Figure 6) is discussed in detail. The difference between the structural frameworks of **16** and **15**·PhMe is a consequence of the similarity between the ionic radii of  $\text{Sr}^{2+}$  and  $\text{Eu}^{2+}$  because the structures of both  $[\text{Sr}_2(\text{Odpp})_4]\cdot\text{PhMe}$ <sup>[17]</sup> and  $[\text{Eu}_2(\text{Odpp})_4]\cdot\text{PhMe}$ <sup>[11]</sup> have the connectivity adopted in **16**. The unusual  $[\text{M}(\mu\text{-OR})_3\text{M}'(\text{OR})]$  core is also observed in the structures of  $[\text{Eu}_2(\text{dme})_3(\text{OAr}^5)_4]$  ( $\text{OAr}^5=2,6\text{-dimethylphenolate}$ )<sup>[32]</sup> and  $[\text{M}[\text{Nd}(\text{Odpp})_4]]$  ( $\text{M}=\text{Na, K}$ ).<sup>[26–28]</sup> As with **15**·PhMe, the metal positions in **16** are disordered (Sr1: Sr/Eu 82:18; Eu1: Eu/Sr 64:36). Therefore, the overall structure of **16** has an excess of Sr over Eu (1.18:0.82). A similar, but less marked Sr/Eu disorder exists in the structure of **16**·PhMe.

The Eu–O bond lengths in **16** range from 2.417(7) to 2.444(9) Å (average 2.43 Å) and are within the range of the Eu–O(bridging) bond lengths in **15**·PhMe (Table 4). They also agree well with the average Eu–O length (2.44 Å) in the  $[\text{Eu}_2(\text{Odpp})_3]^+$  cation of **3** and the average Eu–O(bridging) length (2.44 Å) of Eu2 in  $[\text{Eu}_2(\text{Odpp})_4]\cdot\text{PhMe}$ ,<sup>[11]</sup> which also contains three bridging Odpp ligands. The Sr–O(bridging) bond lengths (2.404(7)–2.622(8) Å) of **16** (average 2.51 Å) are longer than in  $[\text{Sr}_2(\text{Odpp})_4]\cdot\text{PhMe}$  (average 2.46 Å),<sup>[17]</sup> possibly due to the higher coordination number (average 4 vs. 3.5). Although the average Sr–O(bridging) bond length is longer than in **10**·0.5 PhMe (2.45 Å for cation 1), the O–Sr–O angles are similar. The Sr–O (terminal aryloxide) bond length in **16** (2.313(8) Å) is comparable to

the Sr–O (terminal aryloxide) bond length in  $[\text{Sr}_2(\text{Odpp})_4]\cdot\text{PhMe}$  (2.355(2) Å).<sup>[17]</sup>

The coordination spheres of atoms Sr1 and Eu1 in **16** are supplemented by  $\pi$ -Ph–metal interactions from pendant phenyl groups (Table 5). There is an  $\eta^2$ -Ph interaction and two  $\eta^3$ -Ph interactions for Eu1 (Eu–C 3.035(9)–3.236(9) Å). For Sr1, there are two  $\eta^1$ -Ph interactions (Sr–C 3.156(6), 3.293(8) Å). The  $\pi$ -Ph–metal interactions in **16** resemble those of the relevant atoms of  $[\text{Sr}_2(\text{Odpp})_4]\cdot\text{PhMe}$ <sup>[17]</sup> and  $[\text{Eu}_2(\text{Odpp})_4]\cdot\text{PhMe}$ .<sup>[11]</sup>

**The structures of  $[\text{BaSr}(\text{Odpp})_4]$  (17) and  $[\text{BaEu}(\text{Odpp})_4]$  (18):** As a consequence of the comparable ionic radii of  $\text{Sr}^{2+}$  and  $\text{Eu}^{2+}$ ,<sup>[16]</sup> the crystal structures of  $[\text{BaSr}(\text{Odpp})_4]$  **17** and  $[\text{BaEu}(\text{Odpp})_4]$  **18** are very similar, as exemplified by their comparable unit cell parameters (Table S1 in the Supporting Information). The structure of  $[\text{BaEu}(\text{Odpp})_4]$  **18**·PhMe is comparable to that of **18**, but with the addition of a toluene molecule in the crystal lattice and slight differences in the  $\pi$ -Ph–metal interactions (Table 5). The structural frameworks of **17** and **18**, which has a terminal Odpp bound to barium (Figure 6), are comparable to those of **16** and the parent homometallic dimeric compounds  $[\text{M}_2(\mu\text{-Odpp})_3(\text{Odpp})]$  ( $\text{M}=\text{Sr, Ba, Eu}$ )<sup>[11,17]</sup> all having three bridging aryloxide ligands.

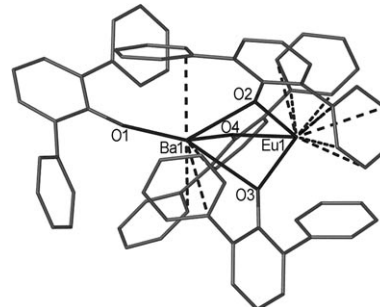


Figure 6. Structure of  $[\text{BaEu}(\text{Odpp})_4]$  (18). Hydrogen atoms are omitted for clarity.

The Ba–O(bridging) bond lengths cover a wide range (2.552(4)–2.917(4) Å in **17**; 2.562(2)–2.940(2) Å in **18**), similarly to the Ba–O(bridging) in  $[\text{Ba}_2(\text{Odpp})_4]$  (difference 0.381 Å).<sup>[17]</sup> This considerable asymmetry in the Ba–O(bridging) bond lengths correlates with a wide range of Sr/Eu–O–Ba angles (Table S2 in the Supporting Information). The largest Sr/Eu–O–Ba angle (98.0(1)° in **17**; 96.95(6)° in **18**) involves the shortest Ba–O(bridging) bond length, whereas the smallest angle (91.2(1)° in **17**; 91.19(6)° in **18**) involves the longest Ba–O(bridging) bond length. Not surprisingly, the terminal Ba–O bond length (2.458(4) Å in **17**; 2.480(2) Å in **18**) is in good agreement with that in  $[\text{Ba}_2(\text{Odpp})_4]$  (2.488(2) Å).<sup>[17]</sup> These are longer than the terminal lengths in the five-coordinate compounds,  $[\text{Ba}(\text{OAr}^4)_2(\text{thf})_3]$ <sup>[33]</sup> (2.38(1) Å and 2.42(1) Å) and  $[\text{Ba}_2(\mu\text{-OCPh}_3)_3(\text{OCPh}_3)(\text{thf})_3]$ <sup>[34]</sup> (2.409(4) Å), therefore, the  $\pi$  bonding (see

below) increases the coordination number effectively as well as formally. Contrasting with the significant range of the Ba–O(bridging) lengths, the Sr–O bond lengths in **17** (2.391(4)–2.505(4) Å) and Eu–O bond lengths in **18** (2.384(2)–2.489(2) Å) span a narrower range and agree with the bridging lengths of the three-oxygen-coordinate Sr atom in  $[\text{Sr}_2(\text{Odpp})_4]\cdot\text{PhMe}$ <sup>[17]</sup> (average 2.44 Å) and the three-oxygen-coordinate Eu atom in  $[\text{Eu}_2(\text{Odpp})_4]\cdot\text{PhMe}$ <sup>[11]</sup> (average 2.44 Å). The bridging Eu–O bond lengths in **18** are slightly shorter than in the heteroleptic complex  $[\text{Eu}_2(\text{dme})_3(\text{OAr}^5)_4]$ <sup>[32]</sup> (2.477(6)–2.597(5) Å), in which Eu has a coordination number of six.

Commensurate with the comparable ionic radii of  $\text{Sr}^{2+}$  and  $\text{Eu}^{2+}$ <sup>[16]</sup> and the similar unit cell parameters of **17** and **18**, the  $\pi$ -Ph–metal interactions in **17** and **18** are similar (Table 5). Thus, there are  $\eta^3$ -Ph–Sr/Eu and  $\eta^5$ -Ph–Sr/Eu interactions involving Sr1 in **17** and Eu1 in **18**. The Sr–C lengths in **17** (3.003(6)–3.285(6) Å) are close to the Eu–C bond lengths in **18** (3.010(3)–3.292(3) Å). There is an  $\eta^2$ -Ph–Ba and two  $\eta^1$ -Ph–Ba interactions at Ba1 in **17** and **18** (Ba–C 3.199(3)–3.388(6) Å) of enough significance to lengthen the terminal Ba–O bond length beyond that in the five-coordinate Ba aryloxide (see above). As in the structures of  $[\text{Sr}_2(\text{Odpp})_4]\cdot\text{PhMe}$ ,<sup>[17]</sup>  $[\text{Ba}_2(\text{Odpp})_4]$ <sup>[17]</sup> and  $[\text{Eu}_2(\text{Odpp})_4]\cdot\text{PhMe}$ ,<sup>[11]</sup> the Ph groups of the terminal Odpp ligand do not participate in  $\pi$  bonding.

**Homometallic structures:** Four homometallic complexes, products of either donor-solvent-induced dissociation or competing reactions in the synthesis of bimetallic complexes, were characterised by X-ray crystallography.

**The structure of  $[\text{Ca}_2(\text{Odpp})_4(\text{thf})_2]$  (**19**):** Dinuclear complex  $[\text{Ca}_2(\text{Odpp})_4(\text{thf})_2]$  **19** (Figure 7) crystallised in the monoclinic space group  $C2/c$ ; half of the molecule resides in the asymmetric unit. Each  $\text{Ca}^{2+}$  metal atom is bound by two bridging aryloxide ligands, a terminal aryloxide ligand and a thf ligand. The coordination geometry around each  $\text{Ca}^{2+}$

atom is best described as distorted tetrahedral. In addition to the  $\sigma$  coordination of the aryloxide and thf ligands, the coordination spheres of the  $\text{Ca}^{2+}$  atoms are supplemented by  $\pi$ -Ph–Ca interactions, that is, there are  $\eta^1$ -Ph and  $\eta^2$ -Ph interactions at each  $\text{Ca}^{2+}$  metal atom. Aside from the presence of ligated thf in **19**, the aryloxo structural frameworks of **19** and  $[\text{Ca}_2(\text{Odpp})_4]\cdot\text{PhMe}$ <sup>[17]</sup> are similar, but the Ca–O aryloxide bond lengths and the  $\pi$ -Ph–Ca interactions differ.

The Ca–Odpp bond lengths in **19** range from 2.236(1) to 2.366(1) Å (average 2.30 Å) for the bridging aryloxide ligands, whereas the Ca–Odpp bond lengths for the terminal aryloxide ligands are shorter (2.153(1) Å). These bond lengths are longer than the Ca–O bond lengths of  $[\text{Ca}_2(\text{Odpp})_4]\cdot\text{PhMe}$ ,<sup>[17]</sup> (Ca–O bridging 2.249(2)–2.275(2) Å, average 2.26 Å; average Ca–O terminal 2.12 Å) owing to the higher (oxygen ligand) coordination number. In contrast to  $[\text{Ca}_2(\text{Odpp})_4]\cdot\text{PhMe}$ ,<sup>[17]</sup> **19** has more unsymmetrical Odpp bridging. The Ca–C lengths for the  $\pi$ -Ph–Ca interactions in **19** range from 3.004(1) to 3.119(1) Å and are within the limits for  $\pi$ -Ph–Ca interactions in  $[\text{Ca}_2(\text{Odpp})_4]\cdot\text{PhMe}$  (3.115(3) Å).<sup>[17]</sup> The additional steric crowding around the  $\text{Ca}^{2+}$  metal atoms in **19** compared with  $[\text{Ca}_2(\text{Odpp})_4]\cdot\text{PhMe}$ <sup>[17]</sup> is exemplified by the absence of  $\pi$ -Ph–Ca interactions from the terminal Odpp ligands, whereas the less crowded, lower (oxygen) coordinate metal environment of  $[\text{Ca}_2(\text{Odpp})_4]\cdot\text{PhMe}$  induces such  $\pi$ -Ph–Ca interactions.

**The structures of  $[\text{Tm}(\text{Odpp})_3]$  (**20**) and  $[\text{Sm}(\text{Odpp})_3]$  (**21**):** The structures of  $[\text{Tm}(\text{Odpp})_3]$  **20** (Figure S1 in the Supporting Information) and  $[\text{Sm}(\text{Odpp})_3]$  **21** both crystallise in the triclinic space group  $P\bar{1}$  and share similar structural features with  $[\text{Ln}(\text{Odpp})_3]$  ( $\text{Ln}=\text{Sc}, \text{La}, \text{Ce}, \text{Pr}, \text{Nd}, \text{Gd}, \text{Ho}, \text{Er}, \text{Yb}, \text{Lu}, \text{Y}$ ).<sup>[29,35–37]</sup> The  $\text{Ln}^{3+}$  metal atom ( $\text{Tm}^{3+}$  in **20** and  $\text{Sm}^{3+}$  in **21**) is bound to three aryloxide ligands and displays trigonal-planar coordination geometry. In addition to the  $\sigma$  coordination of the aryloxide ligands, the coordination sphere of the  $\text{Ln}^{3+}$  metal atom is completed by  $\pi$ -Ph–Ln interactions with the pendant phenyl arms of the aryloxide ligands, which cap the  $\text{Ln}^{3+}$  metal atom above and below the  $\text{LnO}_3$  trigonal plane.

The Tm–O bond lengths in **20** range from 2.045(1) to 2.115(1) Å (average 2.08 Å) and the Sm–O bond lengths in **21** range from 2.129(2) to 2.186(2) Å (average 2.16 Å). After subtracting the relevant ionic radii,<sup>[16]</sup> the average values (1.20 Å in **20** and 1.20 Å in **21**) are comparable to the average Ln–O subtraction bond lengths in  $[\text{Ln}(\text{Odpp})_3]$  ( $\text{Ln}=\text{Nd}$  (1.19 Å),<sup>[37]</sup>  $\text{Yb}$  (1.20 Å)<sup>[29]</sup> and  $\text{Lu}$  (1.19 Å)).<sup>[36]</sup> In **20** and **21** there are  $\eta^1$ -Ph and  $\eta^6$ -Ph interactions with Ln1, which is comparable to the  $\pi$ -Ph–Ln interactions observed in  $[\text{Ln}(\text{Odpp})_3]$  ( $\text{Ln}=\text{Ce}, \text{Pr}, \text{Nd}, \text{Gd}, \text{Ho}, \text{Er}, \text{Yb}, \text{Lu}, \text{Y}$ ).<sup>[29,35–37]</sup> The Ln–C lengths for the  $\pi$ -Ph–Ln interactions in **20** and **21** (2.786(2)–3.051(2) Å and 2.901(2)–3.102(2) Å, respectively) are comparable with analogous Ln–C lengths in  $[\text{Ln}(\text{Odpp})_3]$  ( $\text{Ln}=\text{Ce}, \text{Pr}, \text{Nd}, \text{Gd}, \text{Ho}, \text{Er}, \text{Yb}, \text{Lu}, \text{Y}$ ) after adjustment for ionic radii differences. As seen with the other members of the  $[\text{Ln}(\text{Odpp})_3]$  series, the presence of  $\pi$ -Ph–metal interactions results in elongation of the Ln–O

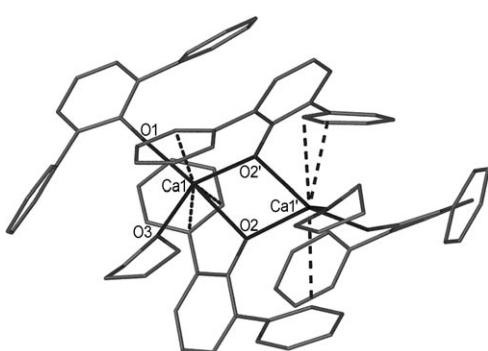


Figure 7. Structure of  $[\text{Ca}_2(\text{Odpp})_4(\text{thf})_2]$  (**19**). Hydrogen atoms are omitted for clarity. Selected bond lengths [Å] and angles [°]: Ca1–O1 2.153(1), Ca1–O2 2.236(1), Ca1–O3 2.332(1), Ca1–O2' 2.367(1), Ca1–C262 3.119(1), Ca1–C21' 3.104(1), Ca1–C212' 3.004(1), O1–Ca1–O2 117.90(3), O1–Ca1–O3 103.07(3), O2–Ca1–O3 116.40(3), O1–Ca1–O2' 156.82(3), O2–Ca1–O2' 75.25(3), O3–Ca1–O2' 85.58(3). Symmetry transformation used to generate equivalent atoms: ' =  $x+1, y, -z+1/2$ '.

bonds of the aryloxide ligands involved in  $\pi$ -Ph–metal interactions to give the relatively large range of Ln–O bond lengths.

*The structure of [Sr(Odpp)<sub>2</sub>(thf)<sub>3</sub>] (**22**):* The Sr<sup>2+</sup> atom of [Sr(Odpp)<sub>2</sub>(thf)<sub>3</sub>] **22** (Figure S2 in the Supporting Information) is bound by two Odpp ligands and three thf ligands, and adopts a distorted trigonal-bipyramidal coordination geometry. Two Odpp ligands reside in the axial positions (O–(Odpp)–Sr–O(Odpp) 164.4(1) $^\circ$ ) and the three thf ligands occupy the equatorial positions (O(thf)–Sr–O(thf) 140.4(1), 139.4(1) and 80.2(1) $^\circ$ ). The distorted trigonal-bipyramidal geometry is emphasised by the O(thf)–Sr–O(Odpp) angles (82.9(1)–102.0(1) $^\circ$ ). Although the stereochemistry of **22** is shared with that of [Sr(OAr<sup>6</sup>)<sub>2</sub>(thf)<sub>3</sub>] (OAr<sup>6</sup>=2,4,6-tri-*tert*-butylphenolate),<sup>[38a]</sup> the latter structure contains two thf ligands in the axial positions and two aryloxide ligands and a thf ligand in the equatorial positions. This is an unexpected stereochemical consequence of the lower crowding in **22** ( $\Sigma$  steric coordination numbers 7.2 and 8.4, respectively).<sup>[38b,c]</sup> The Sr–O(Odpp) lengths in **22** (2.305(3), 2.307(3) Å) are comparable to those in [Sr(OAr<sup>6</sup>)<sub>2</sub>(thf)<sub>3</sub>]<sup>[38a]</sup> (2.32(1), 2.31(1) Å), despite the differences in ligand arrangement. The Sr–O(thf) lengths fall over a wide range (2.471(3)–2.602(3) Å) compared with the corresponding lengths in [Sr(OAr<sup>6</sup>)<sub>2</sub>(thf)<sub>3</sub>]<sup>[38a]</sup> (2.54(1)–2.59(1) Å) and in the aggregate [Sr<sub>4</sub>(HOPh)<sub>2</sub>(OPh)<sub>8</sub>(thf)<sub>6</sub>]<sup>[39]</sup> (2.548(8)–2.584(8) Å). The Sr–O–C<sub>1,19</sub> angles in **22** are slightly bent (157.6(3), 168.7(3) $^\circ$ ), possibly to minimise steric repulsion and to allow close approach of one phenyl ring to Sr1. This phenyl ring sits across the wide O3–Sr–O5 angle (139.4(1) $^\circ$ ) and provides an  $\eta^1$ – $\pi$ -Ph–Sr interaction. The Sr–C length (Sr–C(12) 3.275(4) Å) is in agreement with Sr–C lengths for  $\pi$ -Ph–Sr interactions in [Sr<sub>2</sub>(Odpp)<sub>3</sub>]<sup>+</sup> cations discussed previously.

## Conclusion

The direct reaction of a rare earth metal (Ln) and either a potential divalent rare earth metal (Ln') or an alkaline earth metal (Ae) with HOdpp at elevated temperature gave homoleptic heterobimetallic complexes. The charge-separated [(Ln'/Ae)<sub>2</sub>(Odpp)<sub>3</sub>][Ln(Odpp)<sub>4</sub>] structural class was obtained for a range of metal atoms (Ln'=Yb, Eu; Ae=Ca, Sr, Ba; Ln=Nd, Sm, Ho, Y, Tm, Yb) and the structures demonstrate the similarities between the chemistry of the alkaline earth metals and divalent rare earth metals, with triply Odpp-bridged [(Ln'/Ae)<sub>2</sub>(Odpp)<sub>3</sub>]<sup>+</sup> cations in all structures and low-coordinate [Ln(Odpp)<sub>4</sub>]<sup>–</sup> anions. The heterobimetallic complexes with Ln' or Ae=Ca, Sr are fragmented into homometallic species in thf and are insoluble in non-polar solvents. To overcome this issue, the heterobimetallic complexes were extracted with toluene under pressure at 190°C. In contrast, the complexes with Ae=Ba were successfully recrystallised from toluene/thf. Treatment of [Ba<sub>2</sub>(Odpp)<sub>4</sub>] with [Mg(Odpp)<sub>2</sub>(thf)<sub>2</sub>] in toluene afforded a relat-

ed charge-separated species [Ba<sub>2</sub>(Odpp)<sub>3</sub>][Mg(Odpp)<sub>3</sub>(thf)]. A dinuclear neutral species [AeEu(Odpp)<sub>4</sub>] was obtained when Eu metal and Ca, Sr or Ba metal were reacted with HOdpp, and [BaSr(Odpp)<sub>4</sub>] was prepared similarly. As a result of the absence of donor-solvent co-ligands, the structures of the complex cations [(Ln'/Ae)<sub>2</sub>(Odpp)<sub>3</sub>]<sup>+</sup> and neutral heterobimetallics feature extensive  $\pi$ -Ph–metal interactions with the pendant phenyl groups of the Odpp ligands, which enables the large electropositive metal atoms to attain coordination saturation and steric protection. These results reveal the utility and generality of this metal-based synthetic route for the synthesis of heterobimetallic complexes and establish a new class of charge-separated complexes.

## Experimental Section

The compounds described herein are extremely air and moisture sensitive and consequently all manipulations were carried out by using standard Schlenk line and drybox techniques under an atmosphere of purified nitrogen. Solvents were dried, purified and de-oxygenated by using standard procedures. 2,6-diphenylphenol (HOdpp) and 1,2,4,5-tetramethylbenzene (Aldrich) were used as received. 1,3,5-tri-*tert*-butylbenzene was obtained from Aldrich (Compounds **3–7**, **10**, **11**, **15**, **16**), or prepared according to a literature procedure<sup>[40]</sup> (**12**, **13**, **17**, **18**, **22**). [Ca<sub>2</sub>(Odpp)<sub>4</sub>]-PhMe,<sup>[17]</sup> [Ba<sub>2</sub>(Odpp)<sub>4</sub>],<sup>[17]</sup> [Nd(Odpp)<sub>3</sub>]<sup>[36]</sup> and [Mg(Odpp)<sub>2</sub>(thf)<sub>2</sub>]<sup>[25]</sup> were prepared according to literature procedures, but without activation by mercury for [Ba<sub>2</sub>(Odpp)<sub>4</sub>]. Rare earth metals were obtained as powders from Rhone Poulenc or were freshly filed from chunks (Santoku), and alkaline earth metal turnings or chunks (Aldrich) were similarly treated. Melting points were measured in pipettes sealed under nitrogen, and are uncalibrated. <sup>1</sup>H NMR spectra were recorded by using a Bruker DPX 300 spectrometer and the chemical shifts are referenced to the residual resonances of the solvent. IR spectra (4000–650 cm<sup>–1</sup>) were recorded as Nujol mulls sandwiched between NaCl plates by using a Perkin–Elmer 1600 FTIR spectrometer (**2–11**, **15**, **16**, **19**), or as Nujol mulls sandwiched between KBr plates using a Nicolet IR200 spectrometer (**12–14**, **17**, **18**, **22**). Microanalyses were performed in duplicate by the Campbell Microanalytical Laboratory, University of Otago, Dunedin, New Zealand (**2–11**, **15**, **16**, **19**) or by Complete Analysis Laboratory, Inc., Parsippany, NJ, USA (**12–14**, **17**, **18**; including barium). The neodymium analysis (**6**) was performed by using EDTA titration with a Xylenol Orange indicator<sup>[41]</sup> following the digestion of an accurately weighed sample in concentrated nitric and sulfuric acids and buffering with hexamethylenetetramine.

**Synthesis of charge-separated complexes [(Ln'/Ae)<sub>2</sub>(Odpp)<sub>3</sub>][Ln(Odpp)<sub>4</sub>]:** A lanthanoid metal and ytterbium, europium, calcium, strontium or barium metal and 2,6-diphenylphenol, usually with a flux (1,3,5-tri-*tert*-butylbenzene or 1,2,4,5-tetramethylbenzene) and Hg (2 drops) were sealed under vacuum in a thick-walled Carius tube and then heated under the conditions indicated below. After reaction, the tubes were cooled and opened in the dry-box. In general, the products were either extracted with and recrystallised from toluene at 190°C (for procedure, see below) or, in the case of reactions with barium metal, the products were extracted and recrystallised from toluene/thf. In cases where the sole characterisation was X-ray crystallography of hand-picked single crystals, preparative details are in the Supporting Information (compounds **1**, **4**, **5**, **8**, **9**).

**General procedure for the crystallisation of charge-separated heterobimetallic complexes from toluene at 190°C:** The reaction mixture (consisting of the heterobimetallic complex, unreacted metal and homometallic co-products) was first washed with hexane (50 mL) to remove 1,3,5-tri-*tert*-butylbenzene, then with toluene (50 mL) to remove homometallic co-products. The resulting solid was dried under vacuum, placed in a

Carius tube and covered with a plug of glass wool. Toluene (15 mL) was added to the tube, which was subsequently cooled in liquid N<sub>2</sub>, evacuated and sealed. The tube was then heated at 190°C for 24 h; the vapour pressure exerted by toluene is approximately 7 atm at this temperature. Under these forcing conditions, the heterobimetallic complex was soluble; the tube was carefully inverted while hot so that filtration occurred through the glass wool plug. The tube was then returned to the oven and progressively cooled to ambient temperatures (10°C per day) to afford crystalline materials of the heterobimetallic complexes, often as single crystals of toluene solvates. The Carius tube was opened in the drybox and the crystalline material transferred to a Schlenk flask and dried under vacuum.

**Caution!** H<sub>2</sub> gas is generated during the direct metalation reactions employed in this work. Accordingly, reaction scales must be adjusted to avoid exceeding a pressure of 15 atm when using heavy-walled Carius tubes. Furthermore, when recrystallising the bimetallic complexes from toluene in heavy-walled Carius tubes, the vapour pressure of toluene must not exceed 15 atm and the temperature of the oven should be monitored. Safety precautions, such as using a metal sleeve, must be applied when heating and handling Carius tubes.

#### Synthesis of charge-separated complexes $[(\text{Ln}'/\text{Ae})_2(\text{Odpp})_3][\text{Ln}(\text{Odpp})_4][\text{Yb}_2(\text{Odpp})_3][\text{Y}(\text{Odpp})_4]$ (2)

**Method 1:** Yb metal (0.17 g, 1.0 mmol), Y metal (0.35 g, 4.0 mmol), HOdpp (0.98 g, 4.0 mmol) and Hg (2 drops) were heated at 220°C under vacuum for 5 d. Treatment of the near-insoluble tube contents with toluene (120 mL) at RT gave an orange solution. Filtration, slight evaporation and standing for several days gave a few orange crystals of **2**·PhMe suitable for X-ray crystallography. The dried insoluble material was recrystallised from toluene at 190°C to afford X-ray-quality orange crystals of **2**·0.5PhMe (yield 0.65 g, 59%). (Unit cell:  $P\bar{1}$ ;  $a=16.7025(5)$ ,  $b=23.4531(7)$ ,  $c=25.0191(8)$  Å;  $\alpha=98.056(2)$ ,  $\beta=92.065(2)$ ,  $\gamma=90.447(2)^\circ$ ;  $V=9696.8(5)$  Å<sup>3</sup>). The metal positions of the [Y(Odpp)]<sup>-</sup> anions were disordered Y<sup>3+</sup>/Yb<sup>3+</sup> approximately 70:30. IR (Nujol):  $\tilde{\nu}=1596$  m, 1580 m, 1564 m, 1495 m, 1410 s, 1307 m, 1288 s, 1269 s, 1176 w, 1158 w, 1109 w, 1070 m, 1026 m, 1011 m, 995 w, 929 w, 915 w, 867 m, 852 m, 800 w, 749 s, 730 w, 704 s, 626 cm<sup>-1</sup> m; elemental analysis calcd (%) for C<sub>129.5</sub>H<sub>95</sub>O<sub>7</sub>Y<sub>1</sub>Yb<sub>2</sub> (2198.15): C 70.76, H 4.36; for C<sub>129.5</sub>H<sub>95</sub>O<sub>7</sub>Y<sub>0.7</sub>Yb<sub>2.3</sub> (2223.39; assuming disorder in single crystals applies to the bulk sample): C 69.96, H 4.31; found: C 70.88, H 4.56.

**Method 2:** After a similar synthesis, a small quantity of the reaction mixture was recrystallised from toluene (3 mL) at 190°C by using a small thick-walled glass tube to afford a few orange crystals of **2**·1.5PhMe. (Unit cell:  $P\bar{1}$ ;  $a=16.339(3)$ ,  $b=16.717(3)$ ,  $c=19.081(4)$  Å;  $\alpha=88.88(3)$ ,  $\beta=83.68(3)$ ,  $\gamma=89.18(3)^\circ$ ;  $V=5179(2)$  Å<sup>3</sup>.)

**[Eu<sub>2</sub>(Odpp)<sub>3</sub>][Y(Odpp)<sub>4</sub>] (3):** Eu metal (0.15 g, 1.0 mmol), Y metal (0.36 g, 4.0 mmol), HOdpp (1.0 g, 4.0 mmol), 1,3,5-tri-*tert*-butylbenzene (0.5 g, 2.0 mmol) and Hg (2 drops) were heated at 210°C for 5 d to give a yellow crystalline product interspersed with unreacted metal. A crystal of **3** was hand-picked from the reaction mixture. The reaction mixture was recrystallised from toluene at 190°C to afford bright yellow crystals of **3**·0.5PhMe that were suitable for single-crystal X-ray analysis after drying in vacuo (yield 0.45 g, 43%). IR (Nujol):  $\tilde{\nu}=1597$  m, 1581 m, 1495 m, 1410 s, 1309 m, 1288 s, 1267 s, 1176 w, 1158 w, 1111 w, 1087 m, 1070 m, 1026 m, 1011 m, 994 w, 916 w, 866 s, 850 s, 800 w, 762 s, 749 s, 704 s, 607 cm<sup>-1</sup> s; elemental analysis calcd (%) for C<sub>129.5</sub>H<sub>95</sub>Eu<sub>2</sub>O<sub>7</sub>Y<sub>1</sub> (2155.99): C 72.14, H 4.44; found: C 72.08, H 4.58.

#### [Ca<sub>2</sub>(Odpp)<sub>3</sub>][Nd(Odpp)<sub>4</sub>] (6)

**Method 1:** Ca metal (0.13 g, 3.3 mmol), Nd metal (0.94 g, 6.5 mmol), HOdpp (1.0 g, 4.0 mmol) and Hg (2 drops) were heated at 210°C for 5 d to give a light blue crystalline material and unreacted metal. The reaction mixture was extracted with toluene (100 mL) at RT to give a light blue solution and a blue precipitate. The solution was filtered and concentrated to about 60 mL, then cooled to -20°C to give light blue crystals of [Nd(Odpp)<sub>3</sub>] (Unit cell:  $P\bar{1}$ ;  $a=10.908$ ,  $b=13.0256$ ,  $c=15.5716$  Å;  $\alpha=76.425$ ,  $\beta=87.682$ ,  $\gamma=67.375^\circ$ , in agreement with reported values).<sup>[37]</sup> When the light blue toluene solution containing crystals of [Nd(Odpp)<sub>3</sub>] was stored at -20°C for several weeks, a colour change to dark green

was noted. Dark-green crystals of **6**·PhMe, suitable for single-crystal X-ray analysis, were deposited amongst the light blue crystals.

**Method 2:** Similarly to the synthesis of **3**, Ca metal (0.05 g, 1.2 mmol), Nd metal (0.10 g, 0.7 mmol), HOdpp (1.15 g, 4.7 mmol), 1,3,5-tri-*tert*-butylbenzene (0.5 g, 2.0 mmol) and Hg (2 drops) were heated at 210°C under vacuum for 5 d to give a light blue crystalline material from which the 1,3,5-tri-*tert*-butylbenzene was sublimed to the end of the tube. After extraction with toluene (50 mL) at RT, the reaction mixture was recrystallised from toluene at 190°C to give blue microcrystals of **6**·PhMe (not of X-ray quality), which were dried under vacuum (yield 0.62 g, 48%). M.p. 245–248°C; <sup>1</sup>H NMR (200 MHz, [D<sub>8</sub>]thf, 25°C):  $\delta=12.27^*$  (brs, 6H; *m*-HArO), 10.23\* (brs, 15H; *o*-H(Ph)+*p*-HArO), 7.56 (d, 16H; *o*-H(Ph)), 7.24 (brs, 21H; *m*-H(Ph)+HAr-PhMe), 7.06 (brd, 16H; *p*-H(Ph)+*m*-HArO), 6.42 (brs, 4H; *p*-HArO), 4.03\* (brs, 12H; *m*-H(Ph)), 3.80\*, (brs, 6H; *p*-H(Ph)), 2.36 ppm (brs, 3H; CH<sub>3</sub>-PhMe) (\* denotes Nd<sup>III</sup>); IR (Nujol):  $\tilde{\nu}=1596$  m, 1578 m, 1495 m, 1406 s, 1309 m, 1286 s, 1269 s, 1250 m, 1176 w, 1156 w, 1110 w, 1084 m, 1070 m, 1026 w, 1010 w, 994 w, 914 w, 859 s, 800 w, 767 m, 753 s, 729 m, 702 s, 601 cm<sup>-1</sup> s; elemental analysis calcd (%) for C<sub>126</sub>H<sub>91</sub>Ca<sub>2</sub>Nd<sub>1</sub>O<sub>7</sub> (1941.49; toluene of solvation lost): C 77.95, H 4.72, Nd 7.43; found: C 78.18, H 4.99, Nd 7.58.

The <sup>1</sup>H NMR spectrum of **6**·PhMe is a composite (1:1) of the spectra of [Ca<sub>2</sub>(Odpp)<sub>4</sub>]·PhMe and [Nd(Odpp)<sub>3</sub>], as observed for freshly prepared solutions of these compounds in [D<sub>8</sub>]thf, as follows: [Ca<sub>2</sub>(Odpp)<sub>4</sub>]·PhMe <sup>1</sup>H NMR (200 MHz, [D<sub>8</sub>]thf, 25°C):  $\delta=7.40$  (d,  $J=7.3$  Hz, 16H; *o*-H(Ph)), 7.06 (overlap, t,  $J=7.3$  Hz, 21H; *m*-H(Ph)+HAr-PhMe), 6.90 (overlap, d,  $J=7.3$  Hz, 16H; *p*-H(Ph)+*m*-HArO), 6.30 (t,  $J=7.3$  Hz, 4H; *p*-HArO), 2.18 ppm (s, 3H; CH<sub>3</sub>-PhMe); [Nd(Odpp)<sub>3</sub>] <sup>1</sup>H NMR (200 MHz, [D<sub>8</sub>]thf, 25°C):  $\delta=12.26$  (d,  $J=7.3$  Hz, 6H; *m*-HArO), 10.23 (brm, 15H; *o*-H(Ph)+*p*-HArO), 4.06 (brs, 12H; *m*-H(Ph)), 3.82 ppm (brs, 6H; *p*-H(Ph)).

**Preparative-scale treatment of **6**·PhMe with thf:** A bulk sample of **6**·PhMe from method 2 was extracted with thf (50 mL) to give a bright blue solution. Concentration of the solution to about 20 mL and storage at -10°C for several days gave a mixture of blue and colourless crystals. The former were identified as [Nd(Odpp)<sub>3</sub>(thf)<sub>2</sub>]·2thf (Unit cell:  $P\bar{1}$ ;  $a=10.1112$ ,  $b=21.624$ ,  $c=13.2075$  Å;  $\alpha=90$ ,  $\beta=100.046$ ,  $\gamma=90^\circ$ , in agreement with reported data),<sup>[37]</sup> but the colourless crystals were unsuitable for single crystal X-ray analysis.

**Preparative-scale treatment of **6**·PhMe with toluene/thf:** A sample of **6**·PhMe was suspended in toluene (50 mL) and thf (8 mL) was added dropwise to the reaction mixture with constant stirring to give a blue solution. The solution was filtered and the volume reduced to about 40 mL, which gave colourless crystals of [Ca<sub>2</sub>(Odpp)<sub>4</sub>(thf)<sub>2</sub>] **19** suitable for X-ray crystallography after several days (yield 0.46 g, 38%). <sup>1</sup>H NMR (300 MHz, [D<sub>6</sub>]benzene, 25°C):  $\delta=7.78$  (d,  $J=7.2$  Hz, 16H; *o*-H(Ph)), 7.59–7.55 (m, 8H; *m*-HArO), 7.32 (t, 16H; *m*-H(Ph)), 7.24–7.19 (m, 12H; *p*-H(Ph)+*p*-HArO), 2.55 (brs, 8H; OCH<sub>2</sub>-thf), 1.15 ppm (brs, 8H; CH<sub>2</sub>-thf); IR (Nujol):  $\tilde{\nu}=1596$  s, 1578 s, 1567 m, 1556 m, 1495 s, 1410 s, 1311 s, 1298 s, 1279 s, 1256 s, 1184 w, 1172 w, 1154 m, 1104 w, 1086 m, 1071 s, 1036 s, 1010 m, 994 m, 982 w, 958 w, 942 w, 910 m, 892 m, 861 s, 848 m, 802 m, 754 s, 716 s, 701 s, 884 m, 668 w, 620 m, 612 m, 596 cm<sup>-1</sup> m; elemental analysis calcd (%) for C<sub>80</sub>H<sub>68</sub>Ca<sub>2</sub>O<sub>6</sub> (1205.50): C 79.70, H 5.69; found: C 78.63, H 5.51.

#### [Ca<sub>2</sub>(Odpp)<sub>3</sub>][Ho(Odpp)<sub>4</sub>] (7)

**Method 1:** Similarly to the synthesis of **3**, Ca metal (0.04 g, 1.0 mmol), Ho metal (0.66 g, 4.0 mmol), HOdpp (1.15 g, 4.7 mmol) and Hg (2 drops) were heated at 220°C for 5 d to afford a yellow crystalline material along with unreacted metal. After cooling to RT, a yellow crystal of **7** suitable for X-ray crystallography was hand-picked from the reaction mixture. The presence of [Ho(Odpp)<sub>3</sub>] in the reaction mixture was confirmed by unit cell measurements. (Unit cell:  $P\bar{1}$ ;  $a=10.8713$ ,  $b=13.0768$ ,  $c=15.7451$  Å;  $\alpha=73.9754$ ,  $\beta=87.6061$ ,  $\gamma=67.7917^\circ$ ;  $V=1983.7$  Å<sup>3</sup>, in agreement with data for [Lu(Odpp)<sub>3</sub>]).<sup>[36]</sup>

**Method 2:** The reaction was repeated with Ca metal (0.04 g, 1.1 mmol), Ho metal (0.10 g, 0.6 mmol), HOdpp (0.98 g, 4.0 mmol), 1,3,5-tri-*tert*-butylbenzene (0.50 g, 2.0 mmol) and Hg (2 drops) at 210°C for 5 d. The yellow crystalline material was recrystallised from toluene at 190°C to afford yellow crystals of **7**, which were dried under vacuum (yield 0.31 g,

28%). M.p. 342–348°C; IR (Nujol):  $\bar{\nu}$ =1596 m, 1583 m, 1564 m, 1496 s, 1439 s, 1410 s, 1357 m, 1309 m, 1288 s, 1270 s, 1176 w, 1158 w, 1088 m, 1071 m, 1027 m, 1011 m, 995 w, 927 w, 915 w, 865 s, 854 s, 801 m, 773 m, 750 s, 704 s, 672 w, 626 w, 605 cm<sup>-1</sup> s; elemental analysis calcd (%) for C<sub>126</sub>H<sub>91</sub>Ca<sub>2</sub>Ho<sub>1</sub>O<sub>7</sub> (1962.08): C 77.13, H 4.67; found: C 76.99, H 4.61.

**[Sr(Odpp)<sub>3</sub>][Nd(Odpp)<sub>4</sub>] (10)**: Similarly to the synthesis of 7, Sr metal (0.10 g, 1.1 mmol), Nd metal (0.09 g, 0.6 mmol), HOdpp (0.98 g, 4.0 mmol), 1,3,5-tri-*tert*-butylbenzene (0.5 g, 2.0 mmol), and Hg (2 drops) were heated at 220°C under vacuum for 5 d. The resulting blue-coloured reaction mixture was recrystallised from toluene at 190°C to give blue crystals of **10**·0.5PhMe, which were dried under vacuum (yield 0.41 g, 36%). M.p. >360°C; IR (Nujol):  $\bar{\nu}$ =1596 m, 1580 m, 1560 m, 1495 m, 1406 s, 1357 w, 1311 m, 1284 s, 1268 s, 1176 w, 1158 w, 1110 w, 1085 m, 1070 m, 1026 m, 1012 m, 994 w, 950 w, 928 w, 916 w, 859 s, 849 s, 800 w, 763 s, 749 s, 730 m, 703 s, 668 w, 626 m, 602 cm<sup>-1</sup> s; elemental analysis calcd (%) for C<sub>129.5</sub>H<sub>95</sub>Nd<sub>1</sub>O<sub>7</sub>Sr<sub>2</sub> (2082.65): C 74.68, H 4.60; found: C 74.77, H 4.69.

**[Sr(Odpp)<sub>3</sub>][Ho(Odpp)<sub>4</sub>] (11)**: Sr metal (0.10 g, 1.1 mmol), Ho metal (0.10 g, 0.61 mmol), HOdpp (0.98 g, 4.0 mmol), 1,3,5-tri-*tert*-butylbenzene (0.5 g, 2.0 mmol), and Hg (2 drops) were heated at 220°C under vacuum for 5 d. Recrystallisation from toluene at 190°C afforded yellow crystals of **11**·0.5PhMe (yield 0.37 g, 32%). A unit cell ( $P\bar{I}$ ;  $a$ =16.5268,  $b$ =23.5196,  $c$ =25.0967 Å;  $\alpha$ =82.806,  $\beta$ =89.928,  $\gamma$ =89.833°;  $V$ =9678.30 Å<sup>3</sup>) of a representative crystal established that **11**·0.5PhMe is isomorphous with **10**·0.5PhMe. M.p. >360°C; IR (Nujol):  $\bar{\nu}$ =1597 m, 1582 m, 1561 m, 1495 s, 1410 s, 1357 m, 1308 m, 1286 s, 1270 s, 1176 w, 1158 w, 1111 w, 1080 w, 1070 m, 1026 m, 1012 m, 994 w, 949 w, 926 w, 916 w, 865 s, 850 s, 800 w, 764 s, 749 s, 730 m, 704 s, 627 m, 606 cm<sup>-1</sup> s; elemental analysis calcd (%) for C<sub>129.5</sub>H<sub>95</sub>Ho<sub>1</sub>O<sub>7</sub>Sr<sub>2</sub> (2103.34): C 73.95, H 4.55; found: C 73.74, H 4.65.

#### [Ba<sub>2</sub>(Odpp)<sub>3</sub>][Sm(Odpp)<sub>4</sub>] (12)

**Method 1:** Ba metal (0.14 g, 1.0 mmol), Sm metal (0.15 g, 1.0 mmol), HOdpp (1.00 g, 4.0 mmol), 1,3,5-tri-*tert*-butylbenzene (0.5 g, 2.0 mmol) and Hg (1 drop) were heated at 235°C under vacuum for 7 d to give colourless crystals and a small amount of yellow crystalline material. A colourless crystal of **12** was hand-picked from the reaction mixture, as was a yellow crystal of [Sm(Odpp)] **21**. Extraction of the reaction mixture with toluene/thf (10:3; total volume 33 mL) then reduction of the volume in vacuo to 5 mL gave a green oily solution, which afforded a small number of green crystals of **12**·PhMe suitable for X-ray crystallography on standing overnight.

**Method 2:** Similarly to the synthesis of **12**·PhMe, Ba metal (0.20 g, 1.5 mmol), Sm metal (0.22 g, 1.5 mmol), HOdpp (1.75 g, 7.0 mmol), 1,3,5-tri-*tert*-butylbenzene (0.5 g, 2.0 mmol) and Hg (1 drop) were heated at 225°C for 7 d. Extraction of the reaction mixture with toluene/thf (6:1; total volume 35 mL) followed by reduction of the volume in vacuo to 15 mL afforded green crystals of **12**·4PhMe after 6 days at -20°C (yield 1.0 g, 46%). M.p. 255–260°C; IR (Nujol):  $\bar{\nu}$ =1590 m, 1403 m, 1304 w, 1269 m, 1152 w, 1070 w, 1024 w, 1006 w, 983 w, 860 m, 843 m, 744 s, 691 s, 627 cm<sup>-1</sup> w; elemental analysis calcd (%) for C<sub>126</sub>H<sub>91</sub>Ba<sub>2</sub>SmO<sub>7</sub> (2142.12; toluene of solvation lost): C 71.08, H 4.38, Ba 12.55; found: C 68.54, H 4.65, Ba 12.02.

**[Ba<sub>2</sub>(Odpp)<sub>3</sub>][Yb(Odpp)<sub>4</sub>] (13)**: Ba metal (0.14 g, 1.0 mmol), Yb metal (0.17 g, 1.0 mmol), HOdpp (1.0 g, 4.0 mmol), 1,3,5-tri-*tert*-butylbenzene (0.5 g, 2.0 mmol) and Hg (1 drop) were heated at 235°C under vacuum for 7 d to afford a yellow crystalline material, from which a crystal of **13** was hand-picked. Extraction of the reaction mixture with toluene/thf (4:5; 45 mL) gave an orange solution from which a yellow crystalline solid of **13** precipitated (yield 0.73 g, 59%). IR (Nujol):  $\bar{\nu}$ =1590 m, 1403 s, 1292 m, 1170 w, 1158 w, 1106 w, 1070 w, 1024 w, 1006 w, 873 m, 820 m, 790 m, 744 s, 691 s, 580 cm<sup>-1</sup> m; elemental analysis calcd (%) for C<sub>126</sub>H<sub>91</sub>Ba<sub>2</sub>YbO<sub>7</sub> (2164.71): C 69.91, H 4.24, Ba 12.69; found: C 69.71, H 4.13, Ba 12.56.

**[Ba<sub>2</sub>(Odpp)<sub>3</sub>][Mg(Odpp)<sub>3</sub>(thf)] (14)**: A suspension of [Mg(Odpp)<sub>2</sub>(thf)<sub>2</sub>] (0.33 g, 0.50 mmol) in toluene (20 mL) was added to a stirred suspension of [Ba<sub>2</sub>(Odpp)<sub>4</sub>] (0.31 g, 0.25 mmol) in toluene (20 mL). The heterogeneous mixture was stirred overnight and warmed at 80°C to give an orange-coloured solution, which was then filtered and stored at 0°C and

gave orange crystals of **14** after 2 d (yield 0.12 g, 23%). IR (Nujol):  $\bar{\nu}$ =1584 m, 1496 m, 1403 s, 1321 w, 1286 m, 1222 w, 1164 w, 1070 m, 1030 w, 1000 w, 913 w, 837 s, 808 m, 755 s, 703 s, 604 cm<sup>-1</sup> m; barium analysis calcd (%) for C<sub>112</sub>H<sub>86</sub>Ba<sub>2</sub>MgO<sub>7</sub> (toluene of solvation lost, 1842.80): Ba 14.90; found: Ba 14.66.

**Synthesis of neutral complexes [AeEu(Odpp)<sub>4</sub>] and [BaSr(Odpp)<sub>4</sub>]**: An unsuccessful attempt to prepare [CaSr(Odpp)<sub>4</sub>] that gave [Sr(Odpp)<sub>2</sub>(thf)<sub>3</sub>] is discussed in the Supporting Information.

**[CaEu(Odpp)<sub>4</sub>] (15)**: Ca metal (0.04 g, 1.0 mmol), Eu metal (0.15 g, 1.0 mmol), HOdpp (1.0 g, 4.0 mmol), 1,3,5-tri-*tert*-butylbenzene (0.5 g, 2.0 mmol) and Hg (2 drops) were heated at 210°C for 5 d to give a yellow crystalline material, which was washed with hexane (50 mL) and then extracted with toluene (70 mL) to give a yellow solution. Concentration to 50 mL and standing for several days afforded yellow crystals of **15**·PhMe. The metal positions are disordered approximately 45:55 and 70:30 (Ca/Eu), as observed for several crystals (yield 0.34 g, 27%). M.p. >360°C; IR (Nujol):  $\bar{\nu}$ =1596 m, 1581 m, 1564 m, 1496 m, 1408 s, 1309 m, 1289 s, 1268 s, 1177 w, 1157 w, 1085 w, 1070 m, 1027 w, 1012 w, 994 w, 928 w, 916 w, 861 m, 851 m, 801 w, 763 s, 753 s, 727 m, 703 s, 601 cm<sup>-1</sup> s; elemental analysis calcd (%) for C<sub>72</sub>H<sub>52</sub>Ca<sub>1</sub>Eu<sub>1</sub>O<sub>4</sub> (1173.24; toluene of solvation lost): C 73.71, H 4.47; for C<sub>72</sub>H<sub>52</sub>Ca<sub>1.14</sub>Eu<sub>0.86</sub>O<sub>4</sub> (1249.09; according to disordered composition, toluene of solvation lost): C 75.14, H 4.55; found: C 71.01, H 4.47.

**[SrEu(Odpp)<sub>4</sub>] (16)**: Sr metal (0.09 g, 1.0 mmol), Eu metal (0.15 g, 1.0 mmol), HOdpp (1.0 g, 4.0 mmol), 1,3,5-tri-*tert*-butylbenzene (0.5 g, 2.0 mmol) and Hg (2 drops) were heated at 210°C under vacuum for 5 d to give a yellow crystalline material and unreacted metal. The 1,3,5-tri-*tert*-butylbenzene was sublimed to the end of the tube. A yellow crystal of **16** was hand-picked from the reaction mixture. The two metal positions were disordered approximately 80:20 and 35:65 (Sr/Eu). The tube contents were washed with hexane (50 mL), then extracted in hot toluene (80 mL) to give a yellow solution. Slow-cooling the toluene to RT gave yellow crystals of **16**·PhMe. The two metal positions (Sr/Eu) were disordered approximately 90:10 and 25:75 (yield 0.30 g, 23%). M.p. 170–174°C; IR (Nujol):  $\bar{\nu}$ =1589 m, 1557 m, 1493 m, 1408 s, 1299 m, 1282 s, 1264 m, 1252 m, 1170 w, 1157 w, 1083 w, 1068 m, 1026 w, 1010 w, 992 w, 929 w, 912 w, 849 s, 803 w, 771 w, 759 s, 746 m, 734 m, 709 s, 598 m, 586 cm<sup>-1</sup> s; elemental analysis calcd (%) for C<sub>79</sub>H<sub>60</sub>Eu<sub>1</sub>O<sub>4</sub> (1312.92): C 72.27, H 4.61; for C<sub>79</sub>H<sub>60</sub>Eu<sub>0.87</sub>O<sub>4</sub> (1304.32; according to the single crystal composition): C 72.63, H 4.63; found: C 72.53, H 4.85.

**[BaSr(Odpp)<sub>4</sub>] (17)**: Ba metal (0.28 g, 2.0 mmol), Sr metal (0.18 g, 2.0 mmol), HOdpp (1.0 g, 4.0 mmol), 1,3,5-tri-*tert*-butylbenzene (0.5 g, 2.0 mmol) were heated at 235°C under vacuum for 7 d. A crystal of **17** was hand-picked from the reaction mixture. Extraction of the reaction mixture with toluene/thf (5:1; 25 mL) gave colourless crystals of **17** after 7 d at -20°C (yield 0.26 g, 22%). M.p. 283–286°C; <sup>1</sup>H NMR (300 MHz, [D<sub>8</sub>]thf, 25°C):  $\delta$ =7.65 (s, 16H; o-H(Ph)), 7.24 (t, 16H; m-H(Ph)), 7.07 (t, 8H; m-HArO), 7.00 (d, 8H; p-H(Ph)), 6.36 ppm (brs, 4H; p-HArO); IR (Nujol):  $\bar{\nu}$ =1584 w, 1543 w, 1450 s, 1415 m, 1298 w, 1269 w, 1257 w, 1170 w, 1059 w, 1018 w, 1006 w, 837 s, 802 w, 750 m, 575 cm<sup>-1</sup> m; barium analysis calcd (%) for C<sub>72</sub>H<sub>52</sub>Ba<sub>1</sub>Sr<sub>1</sub>O<sub>4</sub> (1206.10): Ba 11.39; found: Ba 11.52.

#### [BaEu(Odpp)<sub>4</sub>] (18)

**Method 1**: Ba metal (0.14 g, 1.0 mmol), Eu metal (0.15 g, 1.0 mmol), HOdpp (1.0 g, 4.0 mmol), 1,3,5-tri-*tert*-butylbenzene (0.5 g, 2.0 mmol) and Hg (1 drop) were heated at 235°C under vacuum for 7 d. Extraction of the reaction mixture with toluene/thf (6:1; 35 mL) followed by reduction of the volume in vacuo to 20 mL afforded orange crystals of **18** after 2 d at RT (yield 0.74 g, 61%). Barium analysis calcd (%) for C<sub>72</sub>H<sub>52</sub>Ba<sub>1</sub>Eu<sub>1</sub>O<sub>4</sub> (1270.44): Ba 10.81; found: Ba 10.63.

**Method 2**: Similarly, Ba metal (0.28 g, 2.0 mmol), Eu metal (0.30 g, 2.0 mmol), HOdpp (1.0 g, 4.0 mmol) and 1,3,5-tri-*tert*-butylbenzene (0.5 g, 2.0 mmol) were heated at 250°C under vacuum for 7 d. Extraction with toluene/thf (2:1; 30 mL) and cooling to 0°C overnight afforded orange crystals of **18**·PhMe (yield 0.55 g, 43%). M.p. 265–270°C; IR (Nujol):  $\bar{\nu}$ =1596 m, 1543 w, 1491 m, 1403 s, 1316 m, 1275 s, 1164 w, 1147 w, 1053 m, 1030 w, 1024 w, 983 w, 925 w, 855 s, 796 m, 767 s, 697 s, 575 cm<sup>-1</sup> s;

barium analysis calcd (%) for  $C_{72}H_{52}BaEuO_4$ : (1270.49, toluene of solvation lost) Ba 10.81; found: Ba 10.67.

**X-Ray crystallography:** Intensity data were collected by using a Bruker Apex II CCD or an Enraf-Nonius KAPPA CCD with  $Mo_K\alpha$  radiation ( $\lambda=0.7170 \text{ \AA}$ ). Suitable crystals were immersed in viscous hydrocarbon oil and mounted on a glass fibre, which was then mounted on the diffractometer.  $N_t$  (total) reflections were measured by using psi and omega scans and were reduced to  $N_o$  unique reflections, with  $F_o > 2\sigma(F_o)$  being considered to be observed. Data were initially processed and corrected for absorption by using the Apex II program suite<sup>[42]</sup> or the programs DENZO<sup>[43]</sup> and SORTAV.<sup>[44]</sup> The structures were solved by using direct methods and observed reflections were used in least squares refinement on  $F^2$ , with anisotropic thermal parameters refined for non-hydrogen atoms. Hydrogen atoms were constrained in calculated positions and refined with a riding model. Structure solutions and refinements were performed by using the programs SHELXS-97<sup>[45]</sup> and SHELXL-97<sup>[46]</sup> through the graphical interface X-Seed,<sup>[47]</sup> which was also used to generate the figures. Crystal and refinement data are listed in Table S1 in the Supporting Information. CCDC 713749 (**2**·2PhMe), 713750 (**3**), 713751 (3·0.5PhMe), 713752 (**4**), 713753 (**5**), 713754 (**6**·PhMe), 713755 (**7**), 713756 (**9**), 713757 (**10**·0.5PhMe), 713758 (**12**), 713759 (**12**·PhMe), 713760 (**12**·4PhMe), 713761 (**13**), 713762 (**14**), 713763 (**15**·PhMe), 713764 (**16**), 713765 (**16**·PhMe), 713766 (**17**), 713767 (**18**), and 713768 (**18**·PhMe) contains the supplementary crystallographic data for this paper. These data can be obtained free of charge from The Cambridge Crystallographic Data Centre via [www.ccdc.cam.ac.uk/data\\_request/cif](http://www.ccdc.cam.ac.uk/data_request/cif). Variata are given in the Supporting Information.

## Acknowledgements

We are grateful to the Australian Research Council for support and to the Faculty of Science, Monash University, for a Postgraduate Publication Award (to G.J.M.). We gratefully acknowledge support from the National Science Foundation (CHE-0505863, 055273 and 0753807). C.St.P. was supported by a Summer Research Fellowship from Project Advance, Syracuse University. Purchase of the X-ray diffraction equipment at Syracuse was made possible with grants from the National Science Foundation (CHE-9527858), Syracuse University and the WM Keck Foundation.

- [1] a) K. Norton, T. J. Emge, J. G. Brennan, *Inorg. Chem.* **2007**, *46*, 4060; b) M. Moustakimov, M. Kritikos, G. Westin, *Inorg. Chem.* **2005**, *44*, 1499; c) W. J. Evans, M. A. Greci, J. W. Ziller, *Inorg. Chem. Commun.* **1999**, *2*, 530.
- [2] G. B. Deacon, A. Gitlits, B. W. Skelton, A. H. White, *Chem. Commun.* **1999**, 1213.
- [3] P. E. O'Connor, B. Twamley, D. J. Berg, *Inorg. Chim. Acta* **2006**, *359*, 2870.
- [4] J. M. Boncella, T. D. Tilley, R. A. Andersen, *J. Chem. Soc. Chem. Commun.* **1984**, 710.
- [5] a) C. J. Burns, D. J. Berg, R. A. Andersen, *J. Chem. Soc. Chem. Commun.* **1987**, 272; b) C. J. Burns, R. A. Andersen, *J. Chem. Soc. Chem. Commun.* **1989**, 136.
- [6] M. N. Bochkarev, V. V. Khramenkov, Y. F. Rad'kov, L. N. Zakharov, *J. Organomet. Chem.* **1992**, *429*, 27.
- [7] W. J. Evans, K. J. Forrestal, J. W. Ziller, *Polyhedron* **1998**, *17*, 4015.
- [8] a) W. J. Evans, T. A. Ulibarri, *J. Am. Chem. Soc.* **1987**, *109*, 4292; b) M. Nishiura, Z. Hou, Y. Wakatsuki, *Organometallics* **2004**, *23*, 1359.
- [9] a) K. Müller-Buschbaum, C. C. Quitmann, *Eur. J. Inorg. Chem.* **2004**, 4330; b) H. Guo, H. Zhou, Y. Yao, Y. Zhang, Q. Shen, *Dalton Trans.* **2007**, 3555.
- [10] a) A. A. Trifonov, E. A. Fedorova, G. K. Fukin, E. V. Baranov, N. O. Druzhkov, M. N. Bochkarev, *Chem. Eur. J.* **2006**, *12*, 2752; b) D. Freedman, S. Sayan, T. J. Emge, M. Croft, J. G. Brennan, *J. Am. Chem. Soc.* **1999**, *121*, 11713.
- [11] G. B. Deacon, C. M. Forsyth, P. C. Junk, B. W. Skelton, A. H. White, *Chem. Eur. J.* **1999**, *5*, 1452.
- [12] G. D. Smith, P. E. Fanwick, I. P. Rothwell, *Inorg. Chem.* **1989**, *28*, 618.
- [13] C. S. Weinert, P. E. Fanwick, I. P. Rothwell, *Dalton Trans.* **2003**, 1795.
- [14] M. F. Zuniga, G. B. Deacon, K. Ruhlandt-Senge, *Chem. Eur. J.* **2007**, *13*, 1921.
- [15] M. F. Zuniga, G. B. Deacon, K. Ruhlandt-Senge, *Inorg. Chem.* **2008**, *47*, 4669.
- [16] R. D. Shannon, *Acta Crystallogr. Sect. A* **1976**, *32*, 751.
- [17] G. B. Deacon, C. M. Forsyth, P. C. Junk, *J. Organomet. Chem.* **2000**, *607*, 112.
- [18] a) T. P. Hanusa in *Comprehensive Coordination Chemistry II*, Vol. 3 (Eds.: J. A. McCleverty, T. J. Meyer), Pergamon, Oxford, **2004**, p. 1; b) S. Cotton in *Comprehensive Coordination Chemistry II*, Vol. 3 (Eds.: J. A. McCleverty, T. J. Meyer), Pergamon, Oxford, **2004**, p. 93.
- [19] a) T. J. Boyle, L. A. M. Ottley, *Chem. Rev.* **2008**, *108*, 1896; b) K. M. Fromm, *Dalton Trans.* **2006**, 5103; c) N. Y. Turova, *Russ. Chem. Rev.* **2004**, *73*, 1041.
- [20] a) L. G. Hubert-Pfalzgraf, *J. Mater. Chem.* **2004**, *14*, 3113; b) H. C. Aspinall, *Top. Appl. Phys.* **2007**, *53*; c) J. S. Matthews, W. S. Rees, Jr., *Adv. Inorg. Chem.* **2000**, *50*, 173.
- [21] D. C. Bradley, R. C. Mehrotra, I. P. Rothwell, A. Singh, *Alkoxo and Aryloxo Derivatives of Metals*, Academic Press, San Diego, **2001**.
- [22] a) M. N. Bochkarev, *Chem. Rev.* **2002**, *102*, 2089; b) F. G. N. Cloke, *Chem. Soc. Rev.* **1993**, *22*, 17; c) G. B. Deacon, Q. Shen, *J. Organomet. Chem.* **1996**, *511*, 1; d) G. R. Giesbrecht, J. C. Gordon, D. L. Clark, P. J. Hay, B. L. Scott, C. D. Tait, *J. Am. Chem. Soc.* **2004**, *126*, 6387.
- [23] a) K. G. Caulton, M. H. Chisholm, S. R. Drake, K. Folting, J. C. Huffman, *Inorg. Chem.* **1993**, *32*, 816; b) W. J. Evans, D. G. Giarikos, M. A. Greci, J. W. Ziller, *Eur. J. Inorg. Chem.* **2002**, 453.
- [24] W. Maudez, M. Meuwly, K. M. Fromm, *Chem. Eur. J.* **2007**, *13*, 8302.
- [25] M. F. Zuniga, J. Kreutzer, W. Teng, K. Ruhlandt-Senge, *Inorg. Chem.* **2007**, *46*, 10400.
- [26] D. L. Clark, G. B. Deacon, T. Feng, R. V. Hollis, B. L. Scott, B. W. Skelton, J. G. Watkin, A. H. White, *J. Chem. Soc. Chem. Commun.* **1996**, 1729.
- [27] G. B. Deacon, T. Feng, P. C. Junk, B. W. Skelton, A. H. White, *J. Chem. Soc. Dalton Trans.* **1997**, 1181.
- [28] G. B. Deacon, A. Gitlits, P. C. Junk, B. W. Skelton, A. H. White, *Z. Anorg. Allg. Chem.* **2005**, *631*, 861.
- [29] G. B. Deacon, S. Nickel, P. MacKinnon, E. R. T. Tieckink, *Aust. J. Chem.* **1990**, *43*, 1245.
- [30] a) D. M. Barnhart, D. L. Clark, J. C. Gordon, J. C. Huffman, R. L. Vincent, J. G. Watkin, B. D. Zwick, *Inorg. Chem.* **1994**, *33*, 3487; b) R. J. Butcher, D. J. Clark, S. K. Grumbine, R. L. Vincent-Hollis, B. L. Scott, J. G. Watkin, *Inorg. Chem.* **1995**, *34*, 5468; c) J. Hitzbleck, G. B. Deacon, K. Ruhlandt-Senge, *Angew. Chem.* **2004**, *116*, 5330; *Angew. Chem. Int. Ed.* **2004**, *43*, 5218, and references therein.
- [31] K. W. Henderson, G. W. Honeyman, A. R. Kennedy, R. E. Mulvey, J. A. Parkinson, D. C. Sherrington, *Dalton Trans.* **2003**, 1365.
- [32] W. J. Evans, W. G. McClelland, M. A. Greci, J. W. Ziller, *Eur. J. Solid State Inorg. Chem.* **1996**, *33*, 145.
- [33] K. F. Tesh, T. P. Hanusa, J. C. Huffman, C. J. Huffman, *Inorg. Chem.* **1992**, *31*, 5572.
- [34] S. R. Drake, W. E. Streib, K. Folting, M. H. Chisholm, K. G. Caulton, *Inorg. Chem.* **1992**, *31*, 3205.
- [35] G. B. Deacon, P. E. Fanwick, A. Gitlits, I. P. Rothwell, B. W. Skelton, A. H. White, *Eur. J. Inorg. Chem.* **2001**, 1505.
- [36] G. B. Deacon, T. Feng, C. M. Forsyth, A. Gitlits, D. C. R. Hockless, Q. Shen, B. W. Skelton, A. H. White, *J. Chem. Soc. Dalton Trans.* **2000**, 961.
- [37] G. B. Deacon, T. Feng, B. W. Skelton, A. H. White, *Aust. J. Chem.* **1995**, *48*, 741.

- [38] a) S. R. Drake, D. J. Otway, M. B. Hursthause, K. M. A. Malik, *Polyhedron* **1992**, *11*, 1995; b) J. Marcalo, A. P. De Matos, *Polyhedron* **1989**, *8*, 2431; c) G. B. Deacon, T. Feng, B. W. Skelton, A. H. White, *Aust. J. Chem.* **1995**, *48*, 741.
- [39] S. R. Drake, W. E. Streib, M. H. Chisholm, K. G. Caulton, *Inorg. Chem.* **1990**, *29*, 2707.
- [40] J. M. A. Baas, H. Van Bekkum, M. A. Hoefnagel, B. M. Wepster, *Recl. Trav. Chim. Pays-Bas* **1969**, *88*, 1110.
- [41] J. L. Atwood, W. E. Hunter, A. L. Wayda, W. J. Evans, *Inorg. Chem.* **1981**, *20*, 4115.
- [42] Apex II, Version 2.1, Bruker AXS Ltd., Madison, Wisconsin.
- [43] Z. Otwinowski, W. Minor in *Methods in Enzymology*, Vol. 276 (Eds.: C. W. J. Carter, R. M. Sweet), Academic Press, New York, **1997**, p. 307.
- [44] R. H. Blessing, *Acta Crystallogr. Sect. A* **1995**, *51*, 33.
- [45] G. M. Sheldrick, SHELXS-97 Program for crystal structure solution, University of Göttingen, Göttingen, Germany, **1997**.
- [46] G. M. Sheldrick, SHELXL-97 Program for crystal structure refinement, University of Göttingen, Göttingen, Germany, **1997**.
- [47] L. J. Barbour, *J. Supramol. Chem.* **2001**, *1*, 189.

Received: January 27, 2009

Published online: April 9, 2009